CHAPTER (4)

APPARATUS AND EXPERIMENTAL CONDITIONS

All the data reported in this thesis have been measured using Atlas CH-4 mass spectrometer. As in most mass spectrometer, the essential components are :

1. An inlet- system for introducing the sample.
2. An ion source for producing an ion beam.
3. An analyzer by means of which the ion beam can be resolved into its various mass components.
4. A detecting system by means of which the resolved ion beams can be detected.

The description of the mass spectrometer as well as the experimental conditions will be given in the following :

4.1. Conditional Features of the Mass Spectrometer :

An Atlas MAT CH-4 mass spectrometer is a single focusing of 60° magnetic sector analyzer and 224 mm radius of curvature. It is symmetrically arranged such that, the object slit and the image slit are equidistant from the pole boundaries of the magnet. The object slit, the center of curvature of the magnet sector and the image slit lie on a straight line. This model cover the mass number range up to 1200 arranged in three steps 1-100, 1-500, 1-1200.

The apparatus is equipped with an automatic device for changing the slit width such that it allows the following slit combination for ion source and collector $\frac{0.03}{0.9}$, $\frac{0.1}{0.3}$, and $\frac{0.03}{0.07}$.

4.2. Vacuum and Inlet System:-

The ion source region and the analyzer region can be pumped separately. The vacuum system used in conjunction with the mass spectrometer (CH-4) consists of a mechanical fore pump and two mercury diffusion pumps with two liquid nitrogen traps. The pressure in the ion source region is usually better than 1×10^{-5} torr, while in the inlet system the pressure is 1×10^{-5} torr. Figure (3) shows a schematic diagram of the vacuum system together with inlet-system and safety devices.

An inlet system, consisting of six-litter vessel, is used to introduce the (volatile) liquid sample into the ion source. The pressure of the sample, in the tube connecting the sample container to the expansion vessel of the inlet system, can be measured by means of a diaphragm-type capacity torr-meter (MCT). The MCT has a pressure measuring rangee of 0.2 to 5 torr. The sample is introduced into the ion source through a nozzle valve.

In the case of a volatile liquid it must be first outgassed by repeatedly freezing and thawing under vacuum before connecting it to the inlet system as a gas sample. The volume of liquid sample used here is about 0.5 cm^3. If the liquid sample has a low vapor pressure, the whole gas introduction system must be heated. The inlet system of CH-4 mass spectrometer can be heated up to 423K.

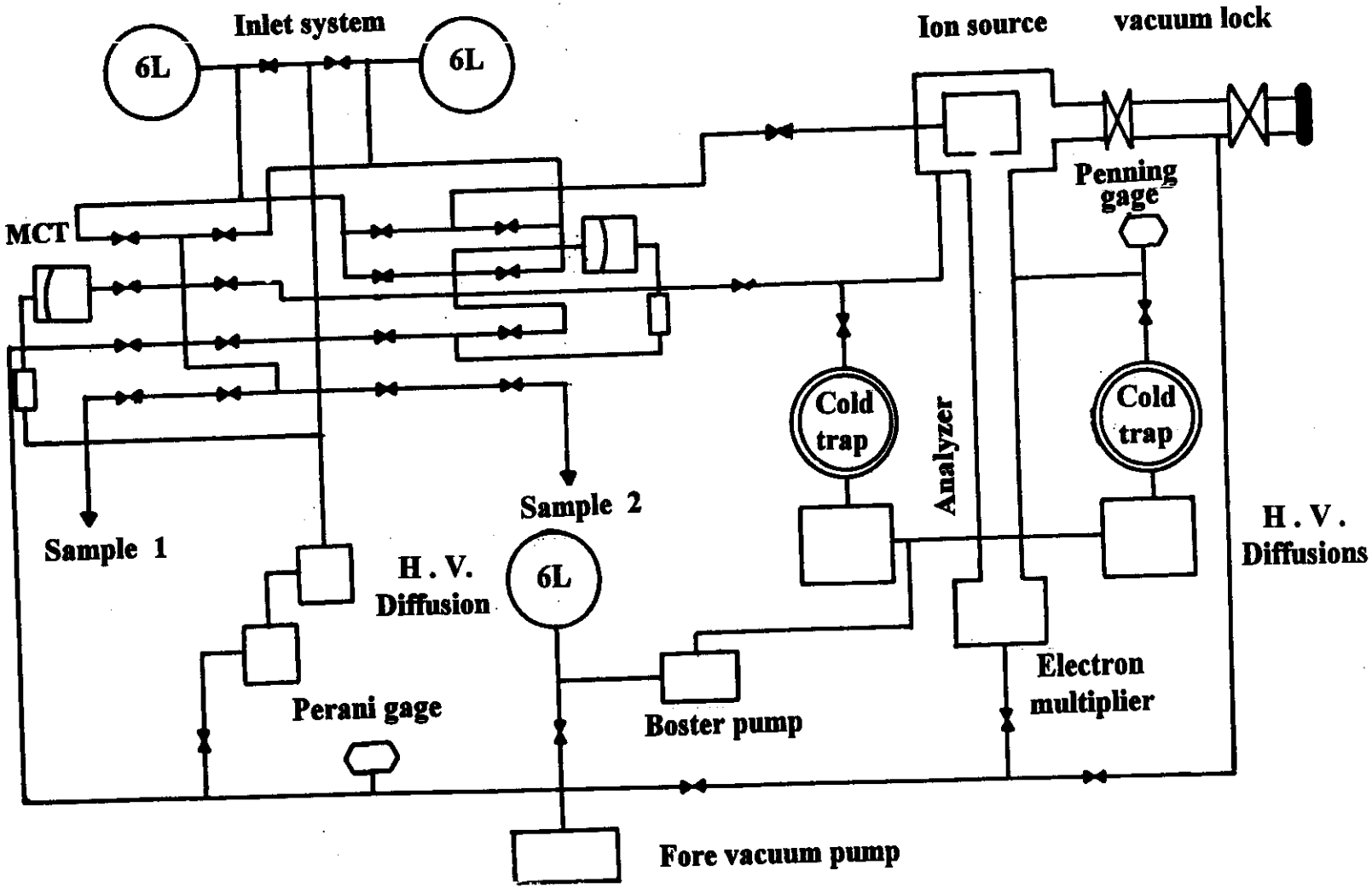

Fig. (3): A schematic diagram of the vacuum system and inlet system.

4.3. Ion Source :

In the present study a gas ion source of the type AN4 is used. A schematic diagram of the ion source AN4 is shown in Figure (4). The electron beam is produced by a cathode filament of Rhenium . The beam is focused by means of an electron lens , on which the potential can be changed between 0 and -6 V relative to the cathode. It is then accelerated into the ionization chamber (k) (Fig. 5) by an energy which can be changed from 0 to 100 eV.

As a result of the electron bombardment with the sample, ionization takes place and the electron beam escapes from the ionization chamber (k) as in Fig.(5), and is trapped by the cathode as an electron collector current and can be measured in this way as the emission current. The current emitted by the cathode (F) can also be measured as the total emission current. The current intensity of the ionizing electron beam can regulated automatically by maintaining the emission current constant through a feedback adjustment voltage. The potential of the collector relative to the ionization region is about +30 V in order to prevent the escape of the secondary electrons.

The ions produced by electron bombardment of the vapor sample are shown out by means of the drawing out plates and are then accelerated into the analyzing tube. The ion accelerating voltage normally used is 3 kV. In order to obtain an optimum ion current, the ion optics must be properly set up by adjusting the voltage on the lens system, deflecting electrodes and drawing out plates. The ion chamber may be operated at temperature up to 673 K.

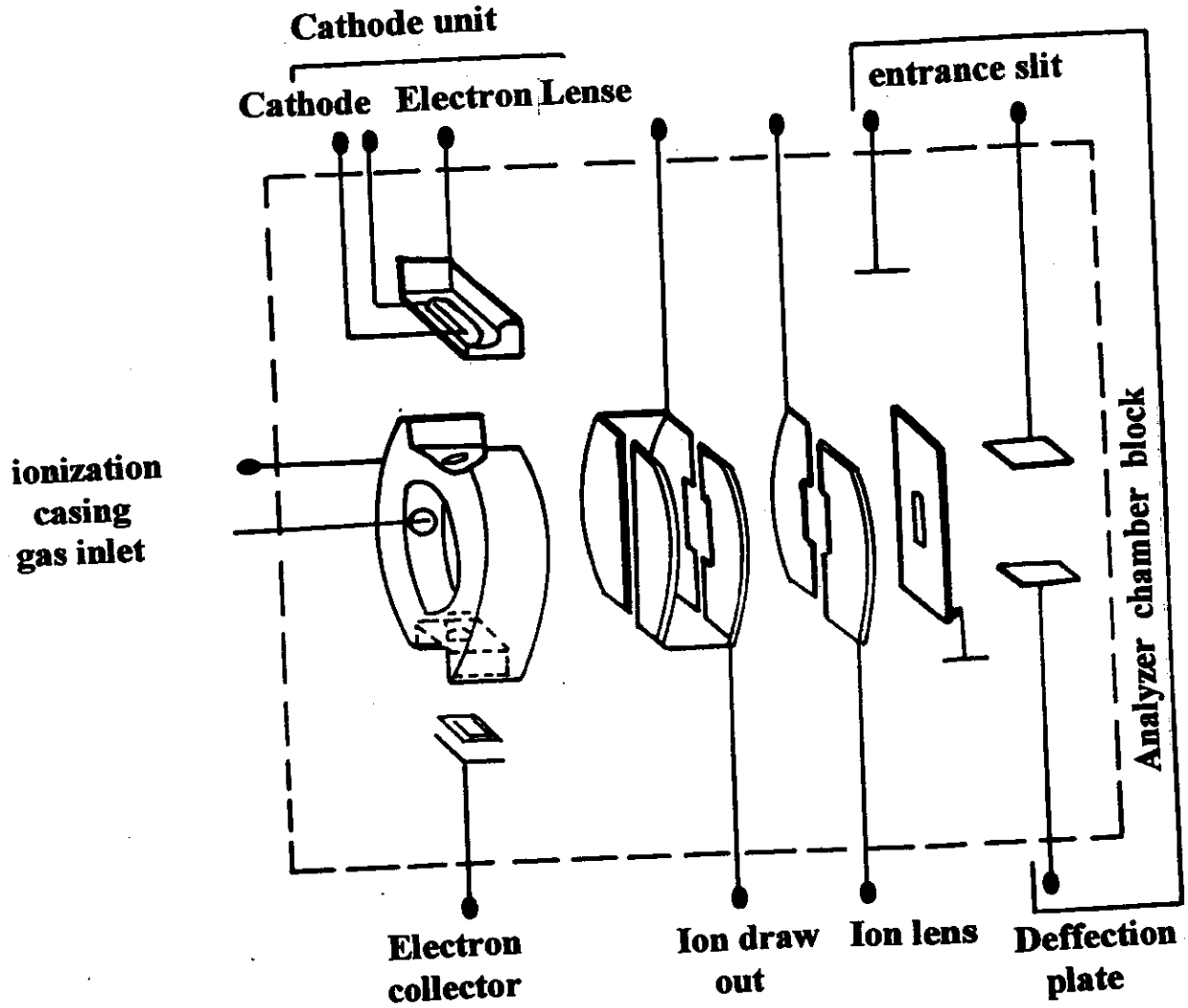

Fig. (4): Ion source AN-4

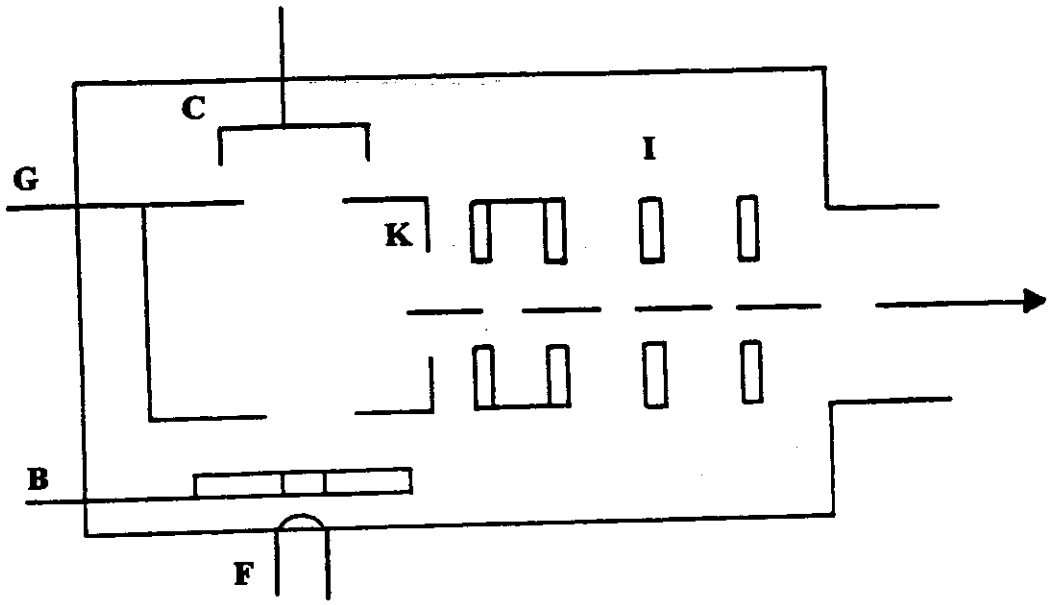

Fig. (5): A Scheme diagram for the ion source AN-4

B-G = Electron Lenses.

K = Ionization chamber.

F = Cathode.

C = Collector.

I = Ion Lense.

4.4. Ion Detection :

The main collector is shaped as electron multiplier, which consists of 17-dynodes, the amplification factor of the electron multiplier is about 10^4. The recorded ion current is about $1x10^{-11}$ up to $3x10^{-6}$ A, depending on the ionization energy and the vapor pressure of the sample.

The intensity of the ions produced corresponding to certain mass numbers can be scanned and recorded over the mass range required. The technique of scanning is performed by means of varying the magnetic current, and in this way a continuous scanning of a very wide mass range is possible. Finally the ion current is detected and recorded by means of a pen-recorder of special type Spedomax G Model S 60000 series.

Argon gas is used in the present study for calibrating the energy scale. The gas is a purified grade and is provided from Matheson Co., Inc., while the amines liquid samples are AR reagents provided from Adwic Laboratory chemicals.

4.5. Operating and Measuring Conditions:

The work performed in this study is done with a pressure of about 1×10^{-5} torr, in the ion source region of the Atlas CH-4 mass spectrometer. The working vacuum, in the analyzer region depending on the vapor pressure of the sample, was better than $1x10^{-6}$ torr. The filament current is set at 4.2A while the emission current is stabilized at about 19 μA . This value of emission current is the lowest value one can obtain when the current has to be stabilized automatically, a condition which is very important in the measurement of ionization efficiency data[35].

The accelerating voltage is 3KV. Electron energy is varied by 0.05 eV step using a 10 turn helipot potentiometer and is measured with digital multimeter model VR- 3115 of Hitachi Ltd.

The temperature of the ion source is kept at ~ 300 K while the inlet system is heated to ~313 K. For the electron multiplier the accelerating voltage is set at 2.5 kV and the gain approximately equals to 1 $x10^4$. The ionization efficiency (IE) curves are obtained by measuring the ion intensity (recorded as peaks on the chart recorder) with the electron energy varied by 0.05 eV steps. The IE curves are measured as fast as possible in order to avoid long-term instrumental drift[130].

To keep the errors in ionization and appearance energy measurements at a minimum, the electron shield potential is set at zero value and the draw out potential is set also at zero value i.e. the ions leak out from the ion gun only under thermal drift. This last condition, although it causes a decrease in ion current, has two advantages[35]. First, avoiding the perturbation of the energy spread of the electron beam and second to increase the residence time of ions in the source. Increasing the residence time of ions favors the detection of low-energy processes and reduces the kinetic shift associated with the fragmentation threshold.

The electron energy is calibrated with argon as a calibrating gas. Argon is introduced together with the sample to be studied into the ionization chamber providing that the currents of the two ions at 70 eV are equal within 10% .The mass spectrometer is baked at about 393 k at the end of the measurement of each ion.

The metastable peaks studied are checked for pressure dependence . Since the analyzer tube pressure in Atlas MAT (CH-4) mass spectrometer could not be determined accurately, the molecular ion peak height is therefore taken as a measure of the analyzer pressure. The results indicated that none of the studied metastable peaks are pressure induced, i.e. they are due to unimolecular dissociations.

CHAPTER (5)

RESULTS AND DISCUSSION

5.1 Results:

5.1.1. Treatment of the Directly Measured Data from the Mass Spectrometer: -

The experimental results are measured as ionization yield (ion current) against ionizing electron energy i.e. ionization efficiency (IE) curve. These directly measured data are treated by the deconvoluted first differential (DFD) technique developed by Selim[5] and applied by Selim et al.[6] by combining the inverse convolution method of Vogt and Pascual[4] with the first differential ionization efficiency (IE) curve.

Since the assumption of Maxwell energy distribution is essential for applying the technique of Vogt and Pascual[4] the present author determined experimentally the energy distribution of the electrons using the second derivative of the Helium IE curves. The results obtained with the presently used ion source (AN-4) show that the distribution of the electrons is Maxwellian within the limits of experimental accuracy. There is no experimental evidence of factors, such as space charge, on the energy distribution of the electrons.

In practice, the deconvolution enhances the random error (noise) of the experimental IE curve, which limits the accuracy of the obtained data and obscures the structure in the IE curve to high extent. In order to eliminate much of the noise in the measured data, each one run

curve is measured of **5** scans of ionizing electron energy. An average curve of 5 scans is obtained and smoothed by a least square fitting method[131] using 5-point smoothing. This method was proved [5,6] to be most effective in discarding noise effects. By comparing smoothed data with unsmoothed data for a number of runs (He, Ar) the author has found that smoothed technique filter much of the random noise without introducing any apparent distortions into the data.

The smoothed data is then treated by a least square[131] cubic equation using 5-point technique to obtain the first derivative (FD) curve. The inverse convolution method of Vogt and Pascual[4] is then applied in order to nullify the effect of a significant portion of the electron energy spread.

Trial calculations performed by using a personal computer model CASIO FP-6000S for IE curves of Ar+ using constants a_1 and a_2 (eq.8. Sec.3.1.3.3) characterising the inverse convolution method[4] of different values corresponding to different temperatures of the filament. The best values are obtained by using $a_1 = -1.40$ and $a_2 = 0.49$. These values are corresponding to temperature T= 1625 K for the filament, $\Delta V = 0.05$eV.

5.1.2. Calculation of the Kinetic Energy ($T_{0.5}$) Release Values

All the metastable peaks reported presently have Gaussion or quasi-Gassion shape. The kinetic energy released ($T_{0.5}$) is calculated from the metastable peak width at half-height (equ.11, Ch.2) after correction for the energy spread in the main ion beam. The corrected width ($d_{1/2}$ corr.) is obtained by the following equation[53] :-

$$d_{1/2}(\text{corr.}) = \sqrt{(d_{1/2})^2_{\text{metastable}} - (d_{1/2})^2_{\text{main beam}}}$$

This equation is exact provided that both metastable peak and main beam have Gaussian profiles. Strictly speaking a mathematical deconvolution procedure should be used[132]. However, the present author used the last equation since it is a satisfactory correction procedure because :

(a) For most metastable peaks, $d_{1/2}$ (main beam) $<< d_{1/2}$ (metastable).

(b) Main beam profiles are approximately Gaussian in shape.

5.1.3. Theoretical Calculations

Calculation of the first ionization energies as well as heats of formation of ethylamine, diethylamine and triethylamine were performed using the standard Modified Neglect of Diatomic Overlap (MNDO) procedure with the associated DFP geometry program[133]. Also, charge distribution on different atoms (neutral and charged parent molecule) is also calculated using the same program.

5.1.4 Tabulation of the Results:

In the present study the author examined the ionization and dissociation of the three molecules namely, ethylamine, diethylamine and triethylamine. Table (1) presents the relative intensities of the different ions in the spectra of the three molecules relative to the base peak at 70 and 14 eV.

The deconvoluted first differential (DFD) ionization efficiency (IE) curves for the molecular ions $[M]^{+\cdot}$, as well as the $[CH_4N]^+$, $[C_2H_6N]^+$ and $[C_3H_8N]^+$ (for diethylamine and triethylamine only) fragment ions obtained from the three molecules are given in Figs (6-16). Most of these curves are

measured up to about 3.5 eV above threshold. Each curve reported is a representative of five curves measured for each ion studied in the present work.. Arrows in the figures show reproducible energy levels observed in the different curves.

The experimentally measured ionization energies at threshold and higher energy levels obtained for the three molecular ions experimentally and determined ΔH_f values together with available similar results reported previously by other authors, using different techniques, are listed in Table(2).

The appearance energy AE at threshold for each fragment ion produced from the three precursors is given in tables (3-5). The tables also contain the processes suggested for the formation of the ions, activation energy (ε_0) calculated thermochemical threshold (ΔE_{th}) values of the different processes as well as excess energy ($\varepsilon_{exc.}$) values.

Values for the heats of formation of the ions, neutral fragments, atoms and molecules used in the calculation of thremochemical threshold (ΔE_{th}) values are given in tables (8 and 9) together with the references from which these values are taken.

Kinetic energy released ($T_{0.5}$) values at 70 eV and 14eV released with metastable peaks are reported in Tables (6 and 7).

Table (1): Electron Impact Mass Spectra of Ethylamine, Diethylamine and Triethylamine (The intensities are given as a percentage to the base peak=100%).

m/z	Ion Formula	R.I					
		ethylamine		diethylamine		triethylamine	
		70 eV	14 eV	70 eV	14 eV	70 eV	14 eV
101	$[C_6H_{15}N]^+$	---	---	---	---	18.13	100
100	$[C_6H_{14}N]^+$	---	---	---	---	5.07	15.77
86	$[C_5H_{12}N]^+$	---	---	---	---	100	76.82
73	$[C_4H_{11}N]^+$	---	---	28.36	100	---	---
72	$[C_4H_{10}N]^+$	---	---	15.67	18.27	2.3	---
58	$[C_3H_8N]^+$	---	---	100	99.5	21.43	37.30
56	$[C_3H_6N]^+$	---	---	2.84	---	5.33	3.55
45	$[C_2H_7N]^+$	29.82	100	0.50	---	0.20	---
44	$[C_2H_6N]^+$	22.96	6.24	26.42	7.77	10.44	1.11
43	$[C_2H_5N]^+$	3.11	1.04	2.45	---	1.78	---
42	$[C_2H_4N]^+$	9.33	0.50	10.90	---	10.60	1.33
30	$[CH_4N]^+$	100	99.8	76.88	41.50	21.20	6.22
29	$[CH_3N]^+$	5.58	0.58	17.32	0.73	11.06	2.22
28	$[CH_2N]^+$	30.41	0.96	23.78	0.83	15.28	2.00
18	$[NH_4]^+$	21.15	1.62	9.07	0.83	3.15	---

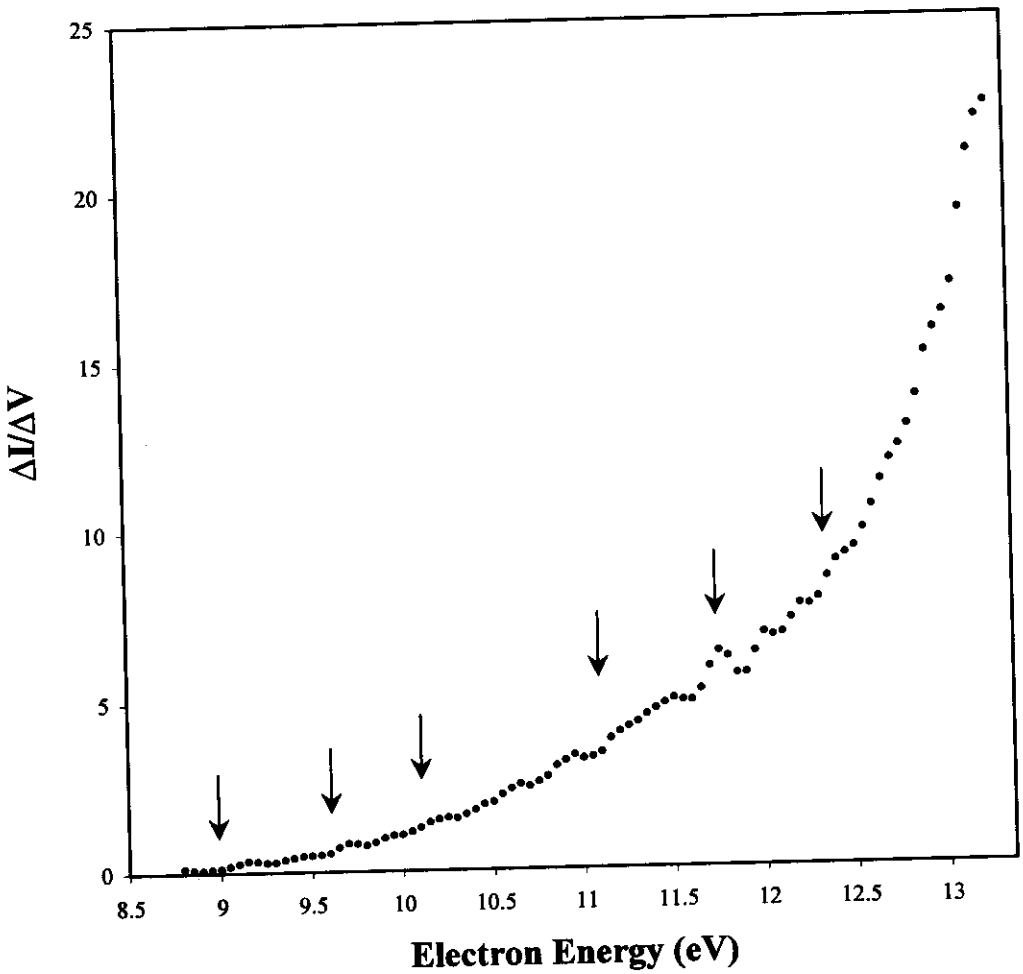

Fig.(6): The DFD IE curve for $[C_2H_7N]^{+\cdot}$ (m/z =45) molecular ion obtained from ethylamine.

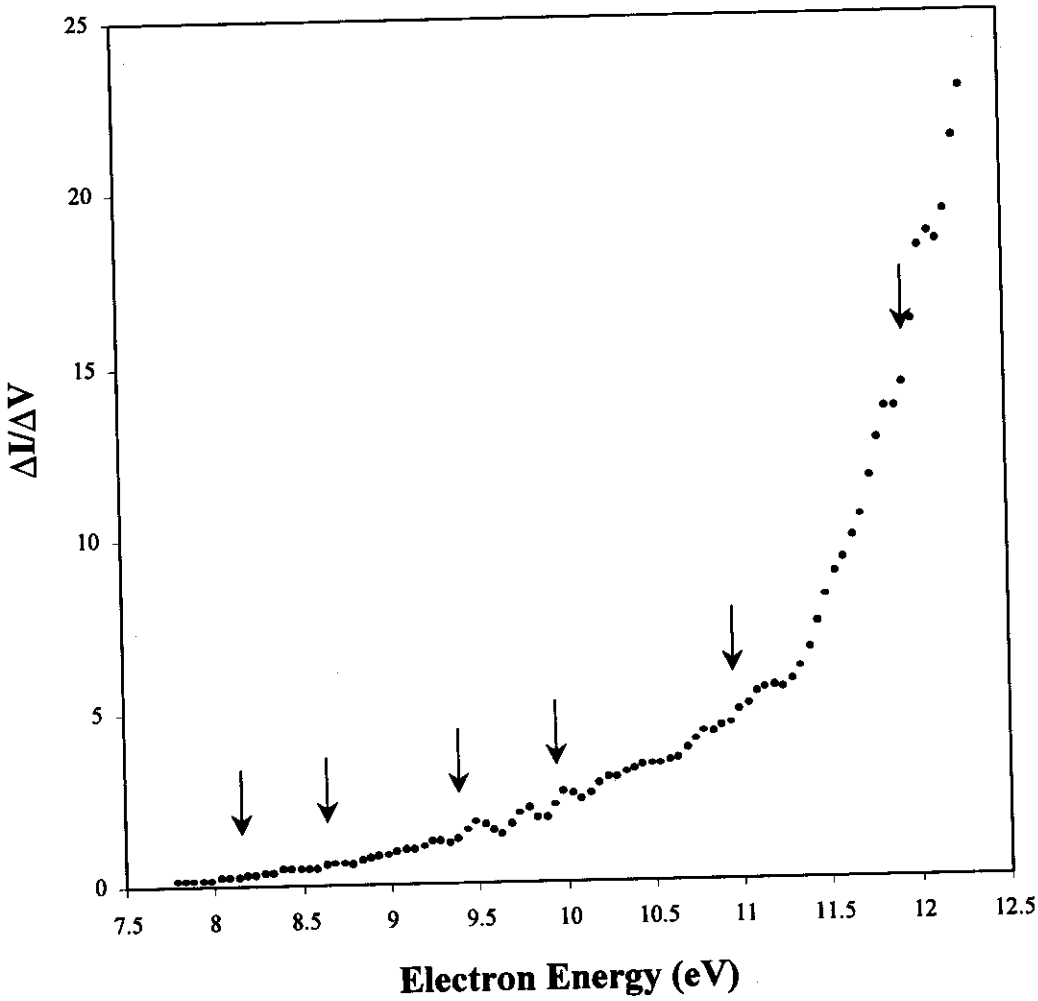

Fig.(7): The DFD IE curve for $[C_4H_{11}N]^{+\cdot}$ (m/z =73) molecular ion obtained from diethylamine.

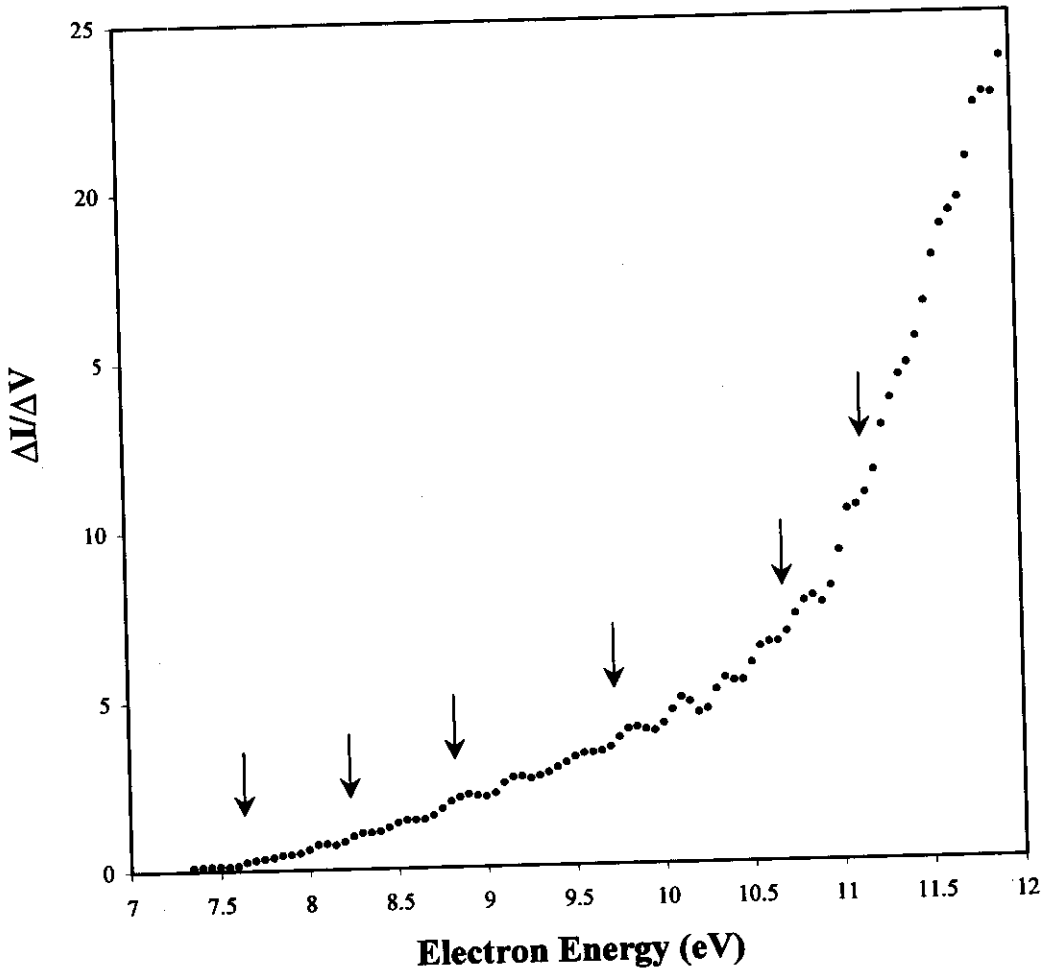

Fig.(8): The DFD IE curve for $[C_6H_{15}N]^{+\cdot}$ (m/z =101) molecular ion obtained from triethylamine.

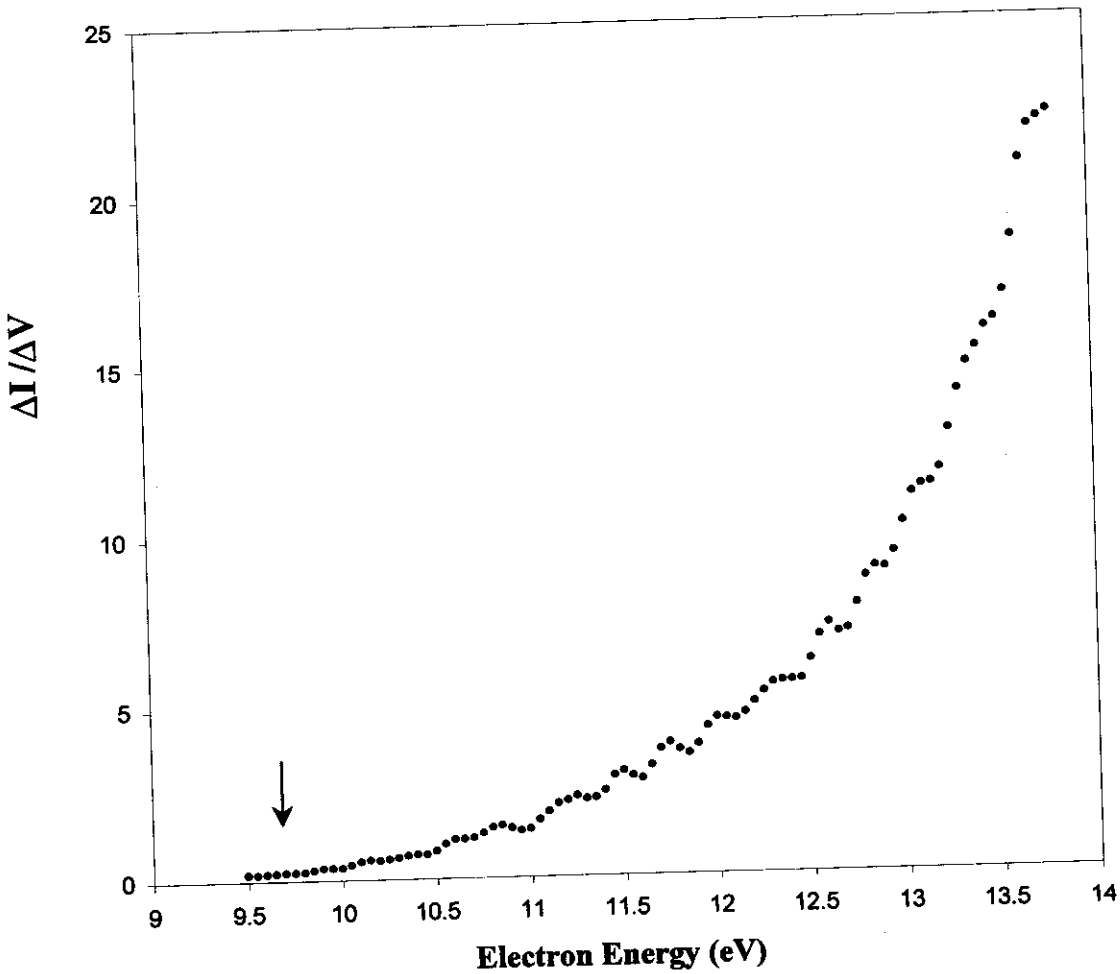

Fig.(9): The DFD IE curve for the fragment $[CH_4N]^+$ (m/z =30) ion obtained from ethylamine.

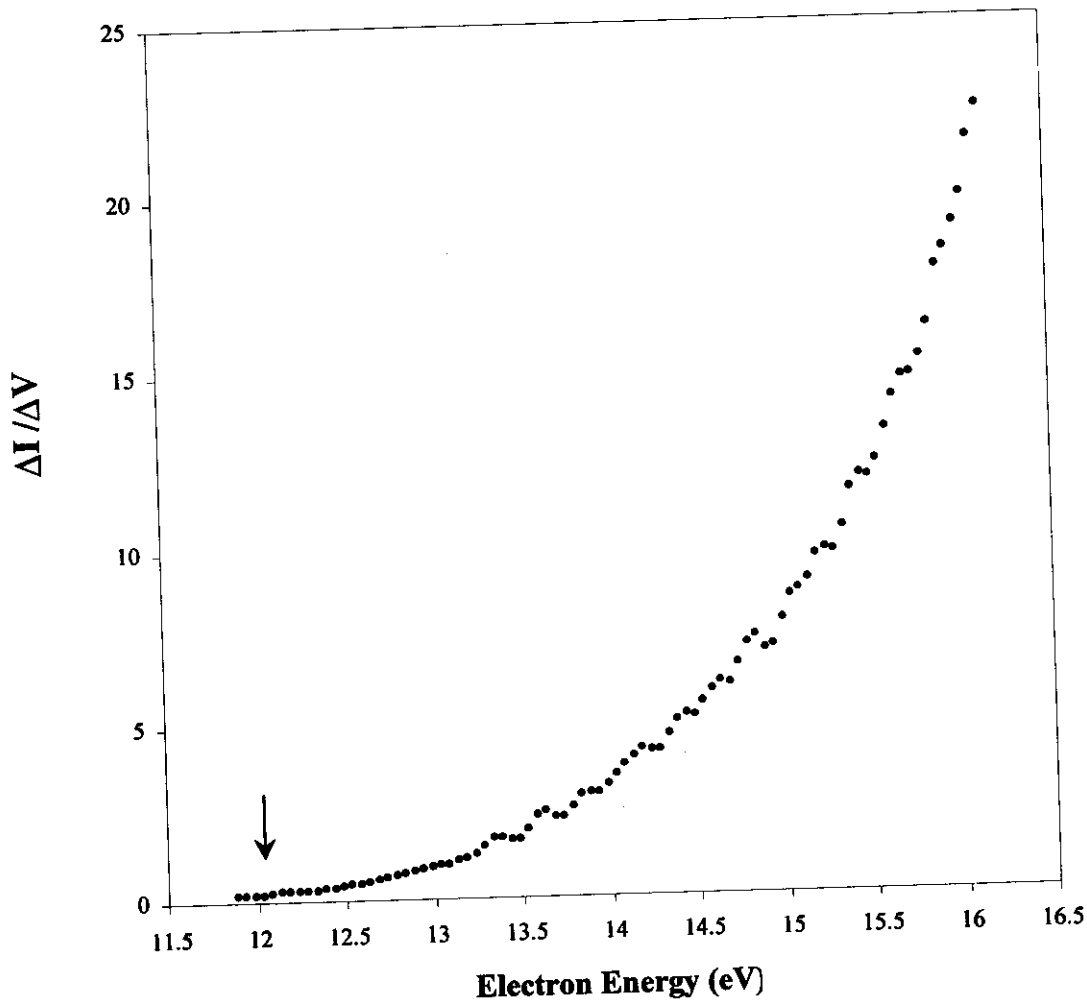

Fig.(10): The DFD IE curve for the fragment $[CH_4N]^+$ (m/z =30) ion obtained from diethylamine.

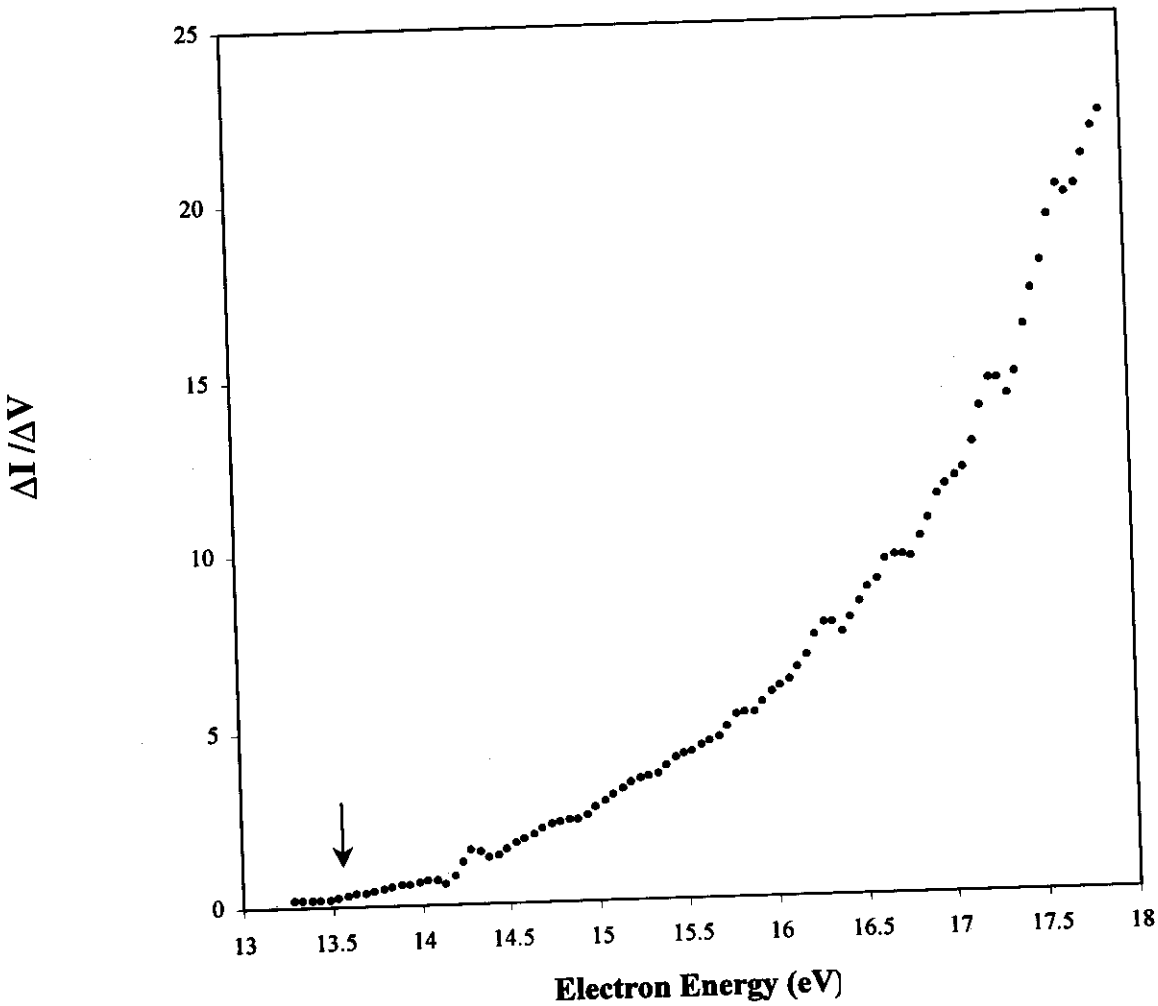

Fig.(11): The DFD IE curve for the fragment $[CH_4N]^+$ (m/z =30) ion obtained from triethylamine.

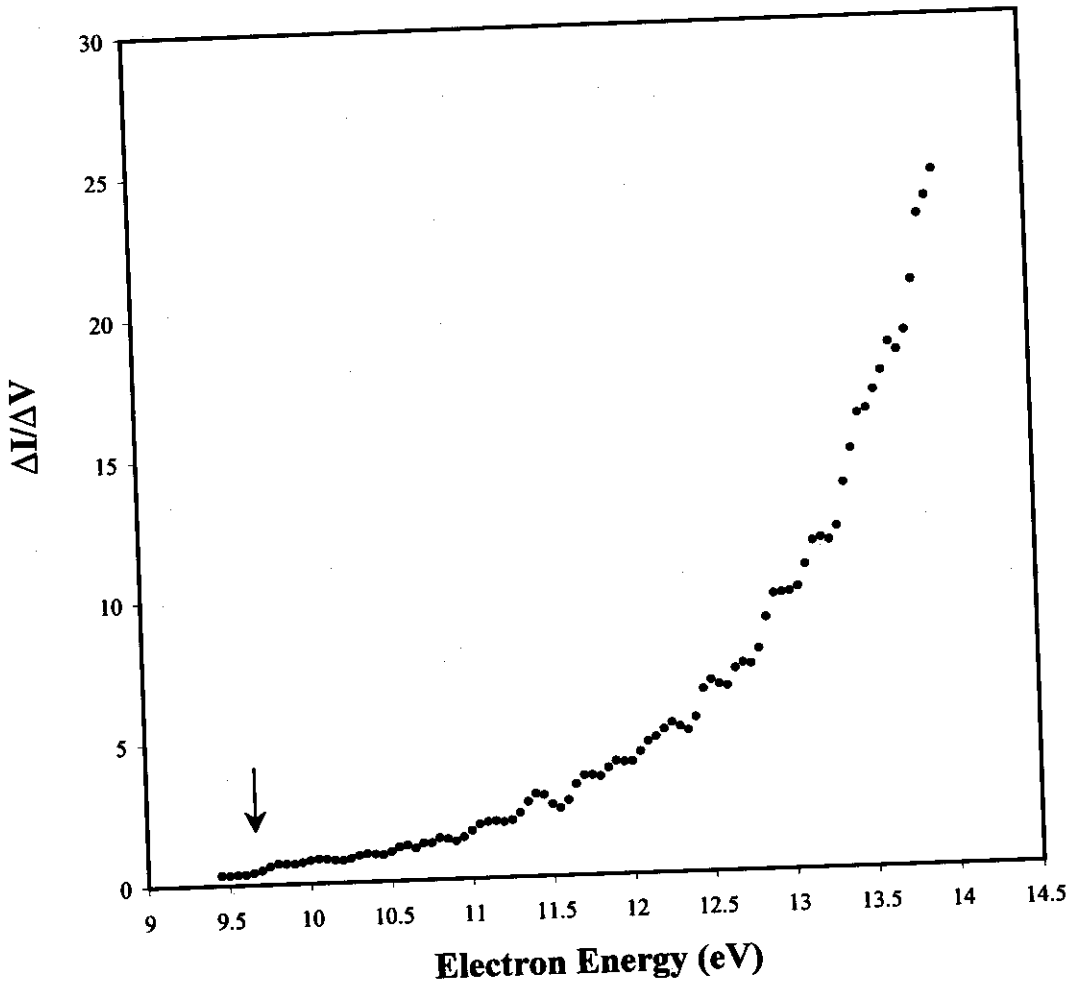

Fig.(12): The DFD IE curve for the fragment $[C_2H_6N]^+$ (m/z = 44) ion obtained from ethylamine

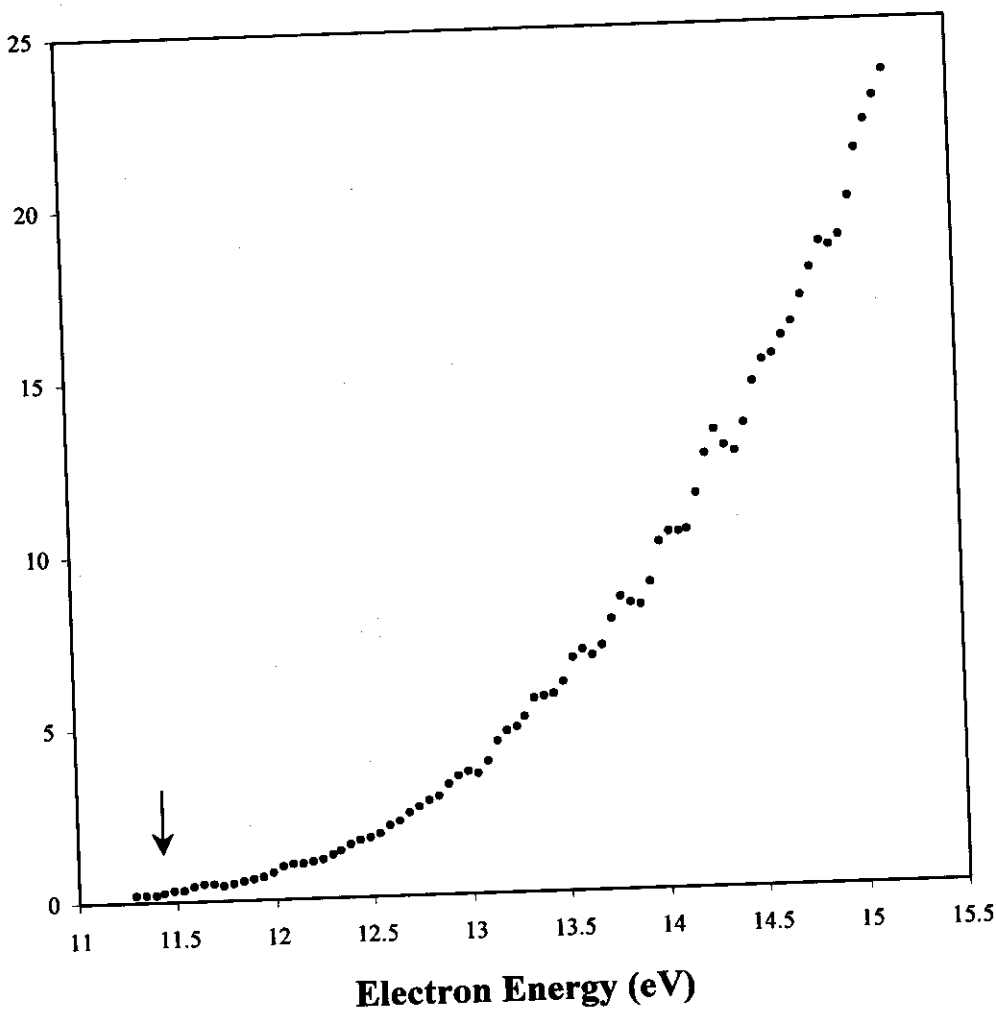

Fig.(13): The DFD IE curve for the fragment $[C_2H_6N]^+$ (m/z = 44) ion obtained from diethylamine.

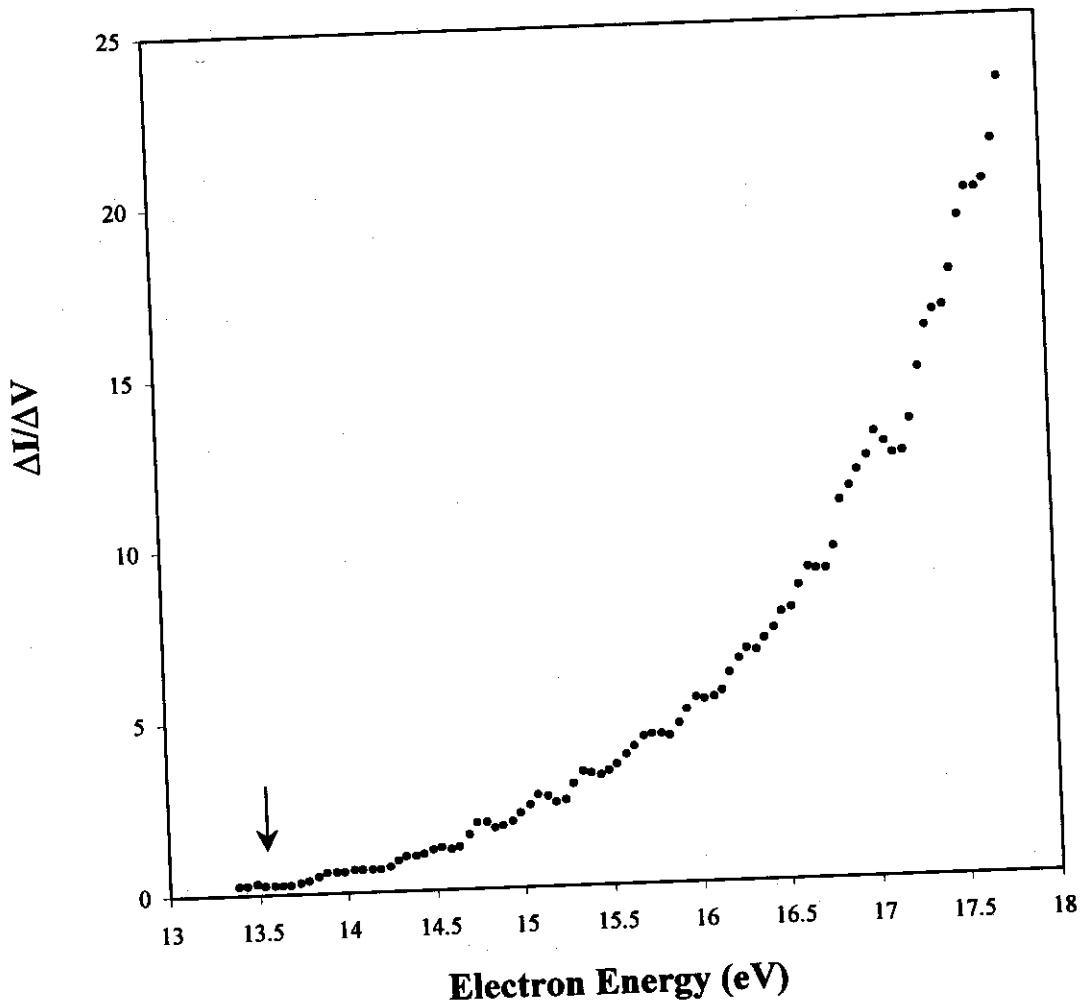

Fig.(14): The DFD IE curve for the fragment $[C_2H_6N]^+$ (m/z = 44) ion obtained from triethylamine.

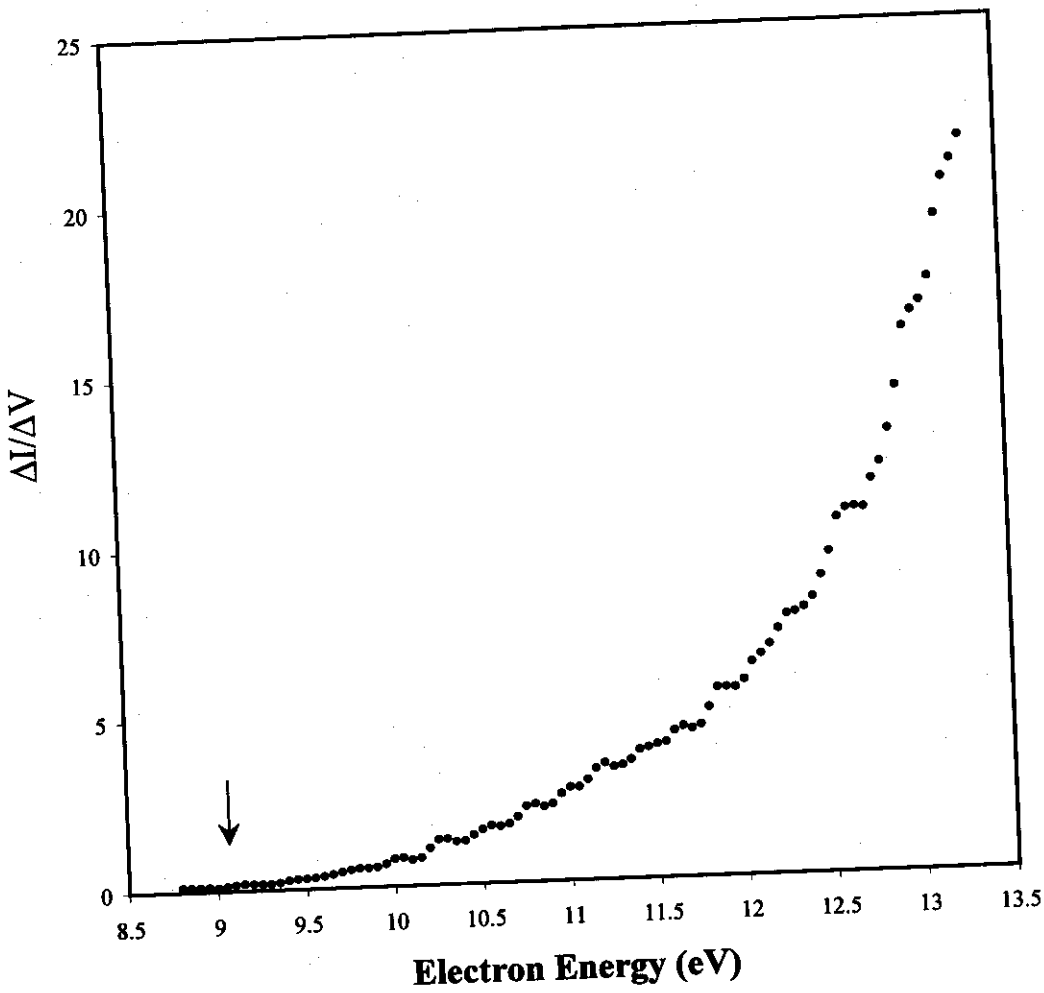

Fig.(15): The DFD IE curve for the fragment $[C_3H_8N]^+$ (m/z = 58) ion obtained from diethylamine

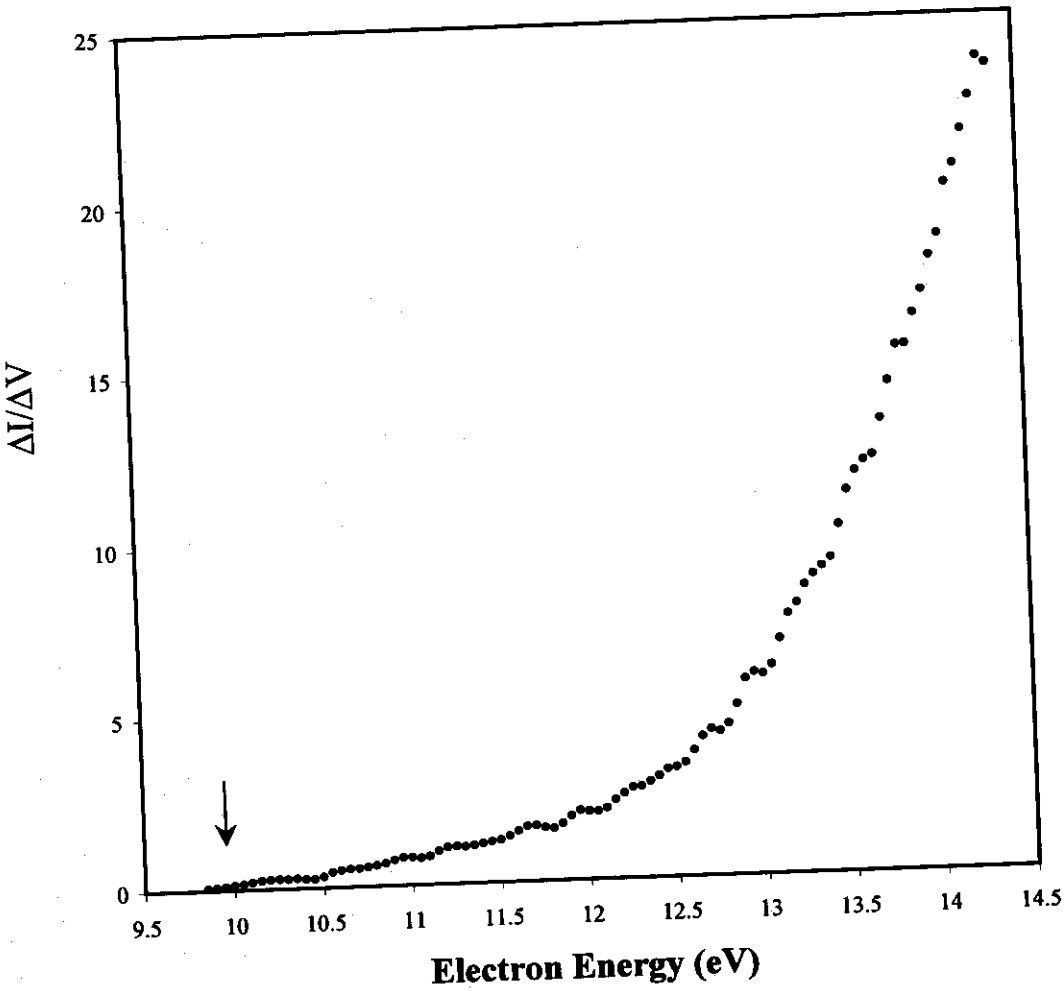

Fig.(16): The DFD IE curve for the fragment $[C_3H_8N]^+$ (m/z = 58) ion obtained from triethylamine

Table (2): Ionization Energies and Heats of Formation ΔH_f Obtained for Ethylamine, Diethylamine and Triethylamine

Molecule	Ionization energy (eV)				ΔH_f (kJ mol^{-1})
	This work	Literature			This work
		EI	PI	PE	
Ethylamine	8.95±0.07	9.19±0.05[10]	8.86±0.02[13]	9.19[14a]	816.04
		9.32[11]			
	9.63±0.10	9.6[9]		---	
	10.2±0.10			---	
	11.14±0.12			---	
	11.80±0.12			11.86[14a]	
	12.52±0.15			12.66[14a]	
	---			14.65[14a]	
	---			15.55[14a]	
	---			16.18[14a]	
Diethylamine	8.15±0.08	8.44±0.01[10]	8.01±0.01[13]	8.51[14a]	713.76
	8.72±0.10			---	
	9.44±0.10	9.5[9]		---	
	10.07±0.10			---	
	11.09±0.12			11.08[14a]	
	11.67±0.12			---	
	---			14.45[14a]	
Triethylamine	7.63±0.07	7.68[12]	7.50±0.02[13]	7.84[14a]	643.38
	8.22±0.09	8.18[12]		---	
		8.55[12] , 7.85±0.07[10]			
	8.88±0.10	8.95[12] , 9.10[9]		---	
		9.40[112]			
	9.83±0.10			---	
	10.68±0.12			10.79[14a]	
	11.19±0.12			---	
	---			14.36[14a]	
	---			15.37[14a]	

Table (3) : Energetics of Production of $[CH_4N]^+$ (m/z =30) Fragment Ions Produced from Ethylamine, Diethylamine and Triethylamine

Molecule	Suggested Processes		Exp. AE (eV)		ε_o (eV)	calculated ΔE_{th} (eV)	ε_{excess} (eV)
			This work	Lit.			
Ethylamine	$[C_2H_7N]^{+\cdot} \rightarrow [CH_4N]^+ + CH_3^{\cdot}$	(1)	9.76± 0.07	9.71[18] 9.96[15] 10.2± 0.10[16]	0.81	9.76[a] 10.54[b]	0 ---
diethylamine	$[C_4H_{11}N]^{+\cdot} \rightarrow [CH_4N]^+ + n\text{-}C_3H_7$	(2)	12.12± 0.07	13.10± 0.10[17]	3.97	9.51[a] 10.43[b]	2.61 1.69
	$\rightarrow [CH_4N]^+ + CH_3 + C_2H_4$	(3)				10.56[a] 11.47[b]	1.56 0.65
Triethylamine	$[C_6H_{15}N]^{+\cdot} \rightarrow [CH_4N]^+ + CH_3 + 2\text{-}C_4H_8$	(4)	13.44± 0.09	---	5.81	10.15[a] 11.06[b]	3.29 2.38
	$\rightarrow [CH_4N]^+ + CH_3 + C_2H_4 + C_2H_4$	(5)				11.31[a] 12.22[b]	2.13 1.22

[a] Methaniminium structure .
[b] Methylnitrinium structure.

N.B. ε_o = Activation Energy (IE - AE)
ΔE_{th} = Calculated thermodynamical threshold using ΔH_f values listed in table 8and 9.
ε_{excess} = Excess energy = AE(exp.) - ΔE_{th}

Table (4) : Energetics of Production of $[C_2H_6N]^+$ (m/z =44) Fragment Ions Produced from Ethylamine, Diethylamine and Triethylamine

Molecule	Suggested Processes		Exp. AE (eV)		ε_0 (eV)	$\Delta E_{th.}$ (eV)	calculated $\varepsilon_{ex.cess}$ (eV)
			This work	Lit.			
Ethylamine	$[C_2H_7N]^{+\cdot} \rightarrow [C_2H_6N]^+ + H$	(1)	9.63±0.09	9.55[15] 9.61 ±0.09[19] 11.9±0.2[16]	0.68	9.59[a] 11.81[c]	0 —
Diethylamine	$[C_4H_{11}N]^{+\cdot} \rightarrow [C_2H_6N]^+ + C_2H_5$	(2)	11.46±0.09	11.42±.0.05[19] 13.65±.0.08[17]	3.31	8.81[a] 10.68[g]	2.65 0.78
	$[C_4H_{11}N]^{+\cdot} \rightarrow [C_2H_6N]^+ + H + C_2H_4$	(3)				10.39[a] 12.26[g]	1.07 —
Triethylamine	$[C_6H_{15}N]^{+\cdot} \rightarrow [C_2H_6N]^+ + H + 2\text{-}C_4H_8$	(4)	13.71±0.07	—	6.08	9.99[a] 12.21[c]	3.72 1.50
	$C_6H_{15}N]^{+\cdot} \rightarrow [C_2H_6N]^+ + H + C_2H_4 + C_2H_4$	(5)				10.90[a] 13.11[c]	2.81 0.60

[a] ethaniminium structure.

[c] β-aminoethyl structure.

[g] $[CH_3CH_2NH]^+$ structure.

Table (5) : Energetics of Production of $[C_3H_8N]^+$ (m/z =58) Fragment Ions Obtained from Diethylamine and Triethylamine.

Molecule	Suggested Processes	Exp. AE (eV) This work	Exp. AE (eV) Lit.	ε_0(eV)	ΔE_{th}(eV)	$\varepsilon_{ex.}$(eV)
Diethylamine	$[C_4H_{11}N]^{+\cdot} \rightarrow [C_3H_8N]^+ + CH_3$ (1)	9.06±0.07	$8.92^{(15)}$	0.91	$8.88^{(a)}$ $9.06^{(b)}$	0.18 0
Triethylamine	$[C_6H_{15}N]^{+\cdot} \rightarrow [C_3H_8N]^+ + n\text{-}C_3H_7$ (2)	9.92±0.09	---	2.29	$8.38^{(a)}$ $8.55^{(b)}$	1.54 1.37
	$\rightarrow [C_3H_8N]^+ + CH_3 + C_2H_4$ (3)				$9.39^{(a)}$ $9.57^{(b)}$	0.53 0.35

[a] $[CH_3CH_2CH{=}NH_2]^+$ structure.

[b] $[CH_3CH_2NH{=}CH_2]^+$ structure.

Table (6) : Metastable Transitions and Kinetic Energy Release ($T_{0.5}$) for Formation and Fragmentation of $[CH_4N]^+$ Ions Obtained from Ethylamine, Diethylamine and Triethylamine.

Molecule	Transition	m*	$T_{0.5}$ (eV)[a]	
			14 (eV)	70 (eV)
Ethylamine	$[CH_4N]^+ \rightarrow [CH_2N]^+ + H_2$	26.1	---	0.280
Diethylamine	$[C_3H_8N]^+ \rightarrow [CH_4N]^+ + C_2H_4$	15.51	0.038	0.038
	$[CH_4N]^+ \rightarrow [CH_2N]^+ + H_2$	26.1	---	0.281
Triethylamine	$[C_3H_8N]^+ \rightarrow [CH_4N]^+ + C_2H_4$	15.51	0.039	0.039
	$[C_5H_{12}N]^+ \rightarrow [CH_4N]^+ + 2\text{-}C_4H_8$	10.5	0.103	---
	$[C_5H_{12}N]^+ \rightarrow [CH_4N]^+ + C_2H_4$	39.1	0.017	---
	$[CH_4N]^+ \rightarrow [CH_2N]^+ + H_2$	26.1	---	0.270

[a] Values of $T_{0.5}$ is the average of four determinations and are reproducible to better than 6%.

Table (7) : Metastable Transitions and Kinetic Energy Release ($T_{0.5}$) for Formation and Fragmentation of $[C_2H_6N]^+$ Ions Obtained from Ethylamine, Diethylamine and Triethylamine.

Molecule	Transition	m*	$T_{0.5}$ (eV)[a]	
			14 (eV)	70 (eV)
Ethylamine	$[C_2H_6N]^+ \rightarrow [NH_4]^+ + C_2H_2$	7.36	---	0.072
Diethylamine	$[C_4H_{10}N]^+ \rightarrow [C_2H_6N]^+ + C_2H_4$	26.89	0.044	---
	$[C_2H_6N]^+ \rightarrow [NH_4]^+ + C_2H_2$	7.36	---	0.079
Triethylamine	$[C_6H_{15}N]^+ \rightarrow [C_2H_6N]^+ + 2\text{-}C_4H_8$	19.36	0.096	---
	$[C_4H_{10}N]^+ \rightarrow [C_2H_6N]^+ + C_2H_4$	26.89	0.042	---
	$[C_2H_6N]^+ \rightarrow [NH_4]^+ + C_2H_2$	7.36	---	0.074

[a] Values of $T_{0.5}$ is the average of four determinations and are reproducible to better than 5% .

Table (8): Heat of formation (ΔH_f) values of neutral species used in the calculation of $\Delta E_{th.}$ values.

Species	ΔH_f (kJ mol^{-1})	Ref.
H	218	136
CH_3	145.8	136
C_2H_4	52.2	136
C_2H_5	118	136
2-C_4H_8	16.9	136
n-C_3H_7	100.5	136
Ethylamine	-50.10	136
Diethylamine	-75.35	136
Triethylamine	-71.93	136

Table (9): Heats of formation (ΔH_f) values of ions used in the calculation of $\Delta E_{th.}$ Values.

Ion	ΔH_f (kJ mol^{-1})	Ref.
$[CH_2= NH_2]^+$	745	136
$[CH_3 - NH]^+$	833	137b
$[CH_3 - CH =NH_2]^+$	657	15
$[CH_2CH_2NH_2]^+$	871	19
$[CH_3CH_2NHCH_2]^+$	653	15
$[CH_3CH_2CHNH_2]^+$	636	15

5.2. Discussion

5.2.1. Fragmentation of Ethylamine, Diethylamine and Triethylamine

Amine spectra[7] tend to be more complex since it is possible to have three-side chains on nitrogen atom. The nitrogen in amines strongly influences the fragmentation pattern observed for this class of compounds[8]. This is due to the low electrophilic character of nitrogen in molecular ion, the nitrogen readily shares its odd electron during homolytic fission of adjacent bonds. A very important fragmentation process is cleavage at the bond β to nitrogen atom, with positive charge remaining on the nitrogen-containing fragment.

The fragmentation producing the most abundant (Table 1)fragment ion (base peak) observed in the mass spectra of the three molecules at 70 eV and 14 eV (except in triethylamine at low energy) are due to β-cleavage (CH_3 rupture from molecular ions). This simple bond cleavage produces the fragment ions $[CH_4N]^+$, $[C_3H_8N]^+$ and $[C_5H_{12}N]^+$ from ethylamine, diethylamine and triethylamine, respectively. This can be reasonably explained from the observation of the charge distribution of positively charged molecular ions at the equilibrium geometry (Fig.17). The electrostatic attraction between nitrogen atom and the α-carbon atom is more than that between nitrogen atom and terminal carbon atoms. Therefor, in this case the C-C bond rupture is much more than the rupture of C-N bonds.

Hydrogen abstraction is also possible and is competitive with the formation of $[M\text{-}CH_3]^+$, the resulting immonium ions are $[C_2H_6N]^+$, $[C_4H_{10}N]^+$ and $[C_6H_{14}N]^+$ from ethylamine, diethylamine and triethylamine,

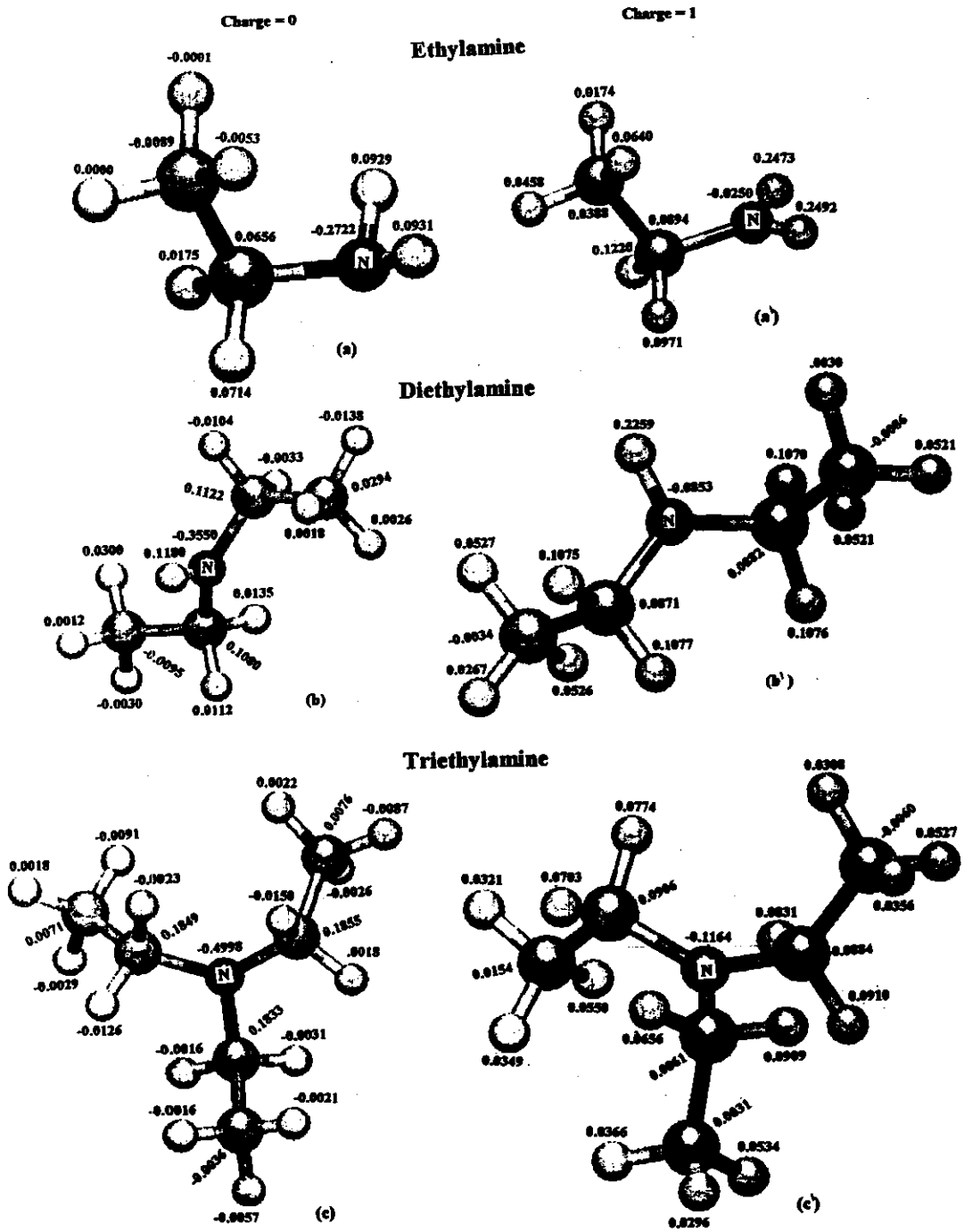

Fig. (18): Charge distribution on different atoms for neutral and cations for ethylamine (a,a'), diethylamine (b,b') and triethylamine (c,c').

respectively. The preferentially loss of CH_3 and H from the molecular ions at 70eV and 14 eV can be illustrated in Table (10): -

Table (10): The abundance ratio of $[M-CH_3]^+$ and $[M-H]^+$ fragment ions from ethylamine, diethylamine and triethylamine.

Molecule	$\frac{[M-CH_3]^+}{[M]^{+\cdot}}$		$\frac{[M-H]^+}{[M]^{+\cdot}}$		$\frac{[M-CH_3]^+}{[M-H]^+}$	
	70 eV	14 eV	70 eV	14 eV	70 eV	14 eV
Ethylamine	3.35	1.0	0.77	0.06	4.35	16.67
Diethylamine	3.53	1.0	0.55	0.18	6.42	5.56
Triethylamine	5.52	0.77	0.30	0.16	18.40	4.81

$[M-CH_3]^+$ and $[M-H]^+$ fragment ions formed from diethylamine and triethylamine can undergo sufficient fragmentation by ethylene exclusion followed by H-migration (α-cleavage from diethylamine and $\alpha+\alpha$ cleavage from triethylamine) to generate an even electron species i.e., $[CH_4N]^+$ and $[C_2H_6N]^+$ ions. H-migration occur from one hydrogen atom of methyl group, since alkene expulsion from labeled ion of structure $CH_2 = NH-CH_2 - CD_3$ show elimination of $C_2D_2H_2$ not $C_2H\,D_3$[134] .

The metastable peaks observed in the mass spectrum for the formation of different important fragment ions can be summarized in schemes 1-3.

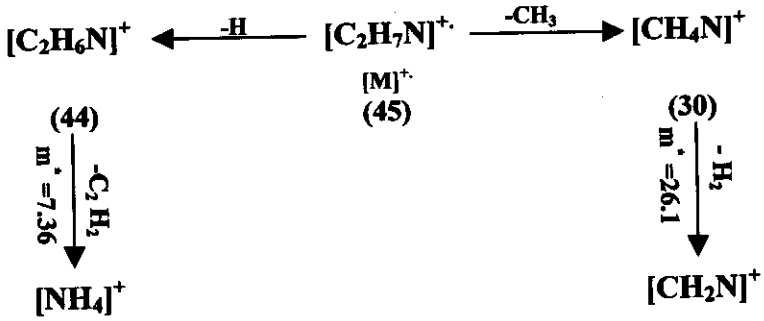

Scheme (1)

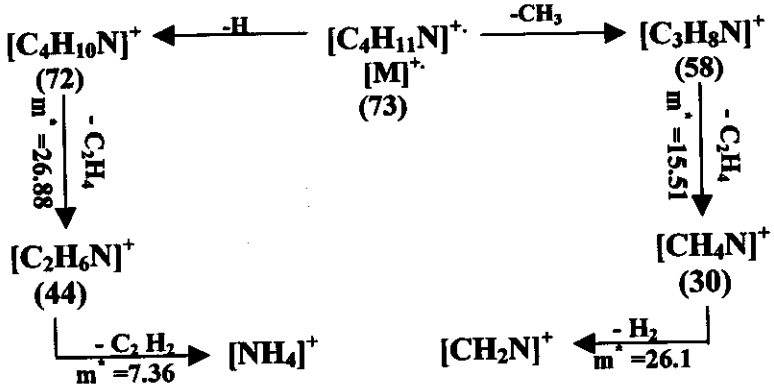

Scheme (2)

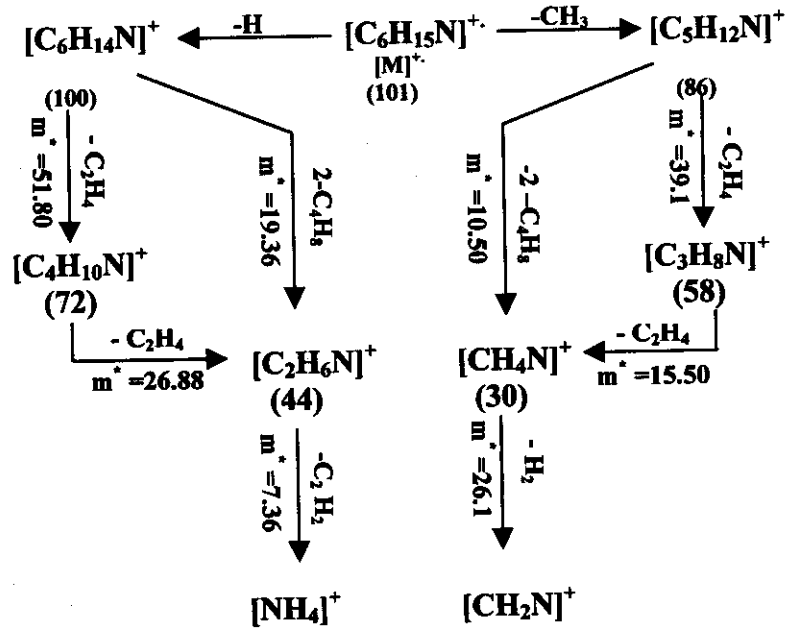

Scheme (3)

Fig.(18) : Schematic diagram of fragmentation pathways for the formation of immonium ions obtained from ethylamine, diethylamine and triethylamine

5.2.2. Molecular Ion

The abundance of the molecular ion, $[M]^{+\cdot}$, depends mainly on its stability and the amount of energy needed to ionize the molecule. Particular structure features tend to show characteristic values of these properties, so that the magnitude of $[M]^{+\cdot}$ provides an indication of the structure of the molecule[135].

Molecular Ions Obtained from Ethylamine, Diethylamine and Triethylamine:

The molecular ions obtained from the three precursors represent the base peak at low energy (14 eV). At 70 eV ethylamine and diethylamine have moderate intensity, while for triethylamine have low intensity (Table1), indicating high stability for the molecular ion at the lower energy than at the higher energy. The DFD IE curves (Fig. 6-8) for the molecular ions show a sharp rise (for about 1 eV above threshold) which may indicate that adiabatic ionization energy coincide with vertical ionization energy. The values of ionization energies reported at threshold are 8.95±0.07 eV (ethylamine),8.15±0.08eV(diethylamine) and 7.63±0.07 eV (triethylamine).

It is evident, from the calculated charge density localized on nitrogen atoms (neutral and charged) (Fig. 17) that the non – bonding orbitals available on nitrogen atom are the site of electron expulsion upon ionization[8]. On the other hand, the charge density on nitrogen atoms in the molecule is decreasing from – 0.2722 to – 0.355 to - 0.4998 for ethylamine, diethylamine and triethylamine, respectively, i.e. the negative charge on nitrogen atom increases with increasing the branching in the

amine. It appears that the ionization energy (IE) value increases with increasing the negative charge on the nitrogen atom.

The presently experimental values of ionization energies at threshold are in a good agreement with that obtained by Watanabe and Mottel[13]using photoionization technique and is lower by about 0.25 eV than the value reported by Collin[10] using electron impact technique (Table2). On the other hand the difference between the values of ionization energies at threshold of ethylamine and triethylamine (1.32 eV) are in a good agreement with the values recorded by Watanabe and Mottle[13] (1.36eV) and by Collin[10] (1.34 eV). The early electron impact measured by Collin[9] for the first ionization energies at 9.6, 9.5 and 9.1 eV for ethylamine, diethylamine and triethylamine, respectively, are higher than the presently measured values, these higher values may not correspond to first ionization energy but higher one (Table 2). On the other hand the first ionization energy and higher energy levels for triethylamine were measured by Melton and Hamill[12] using RPD technique, the present value at 7.63 eV is in agreement with the first ionization energy at 7.68 eV and some presently measured energy levels at 8.22 and 8.88 eV are comparable with measured values at 8.18 and 8.95 eV by Melton and Hamill[12].

The measurement of molecular ionization energies based on photoelectron spectroscopy has been studied by a number of workers[14]. The presently ionization energies values are compared with the early work of Al-Joboury and Turner[14a] pioneering in this field, for their systematic study of the three species (Table 2). The presently measured values of the first ionization energy are lower by about 0.27eV than the measured values by them. Three energy levels observed in the presently measured data at

9.63 eV, 10.20 eV and 11.14 eV (ethylamine), 8.72 eV, 9.44 eV and 10.07 eV (diethylamine) and 8.22 eV, 8.88 eV and 9.83 eV (triethylamine) are not accessible in the photoelectron energy spectra, while some of the presently energy levels at 11.80eV and 12.52eV (ethylamine), 11.09 eV (diethylamine) and 10.68 eV(triethylamine) are in agreement with the measured values at 11.86eV and 12.66 eV (ethylamine), 11.08eV(diethylamine) and 10.79eV(triethylamine) by Al-Joboury and Turner[14a] .

5.2.3. $[CH_4N]^+$ (m/z=30) Fragment Ion

$[CH_4N]^+$ (m/z 30) fragment ion is well known[135] in the mass spectral fragmentation of amines, and is formed from primary amine as a result of homolytic fission (β-cleavage)[8]. Secondary and tertiary amines can also undergo cleavage accompanied with rearrangement eliminating an olefin to generate the ion of m/z 30[8] . The ion exists in two stable forms: the most stable is the methaniminium $[CH_2NH_2]^+$ ion (a)[15,136], and the less stable structure is the methylnitrinium $[CH_3NH]^+$ ion (b)[137]. Much higher theoretical estimates for $\Delta H^\circ_{f,298}$ (b) values have been reported[138].

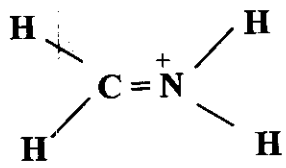

(a)

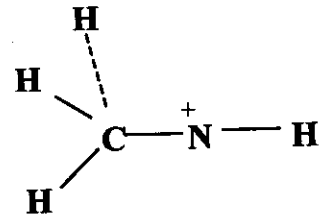

(b)

The $[CH_4N]^+$ fragment ion represents the base peak in the mass spectrum of ethylamine at 70 eV as well as 14 eV, while the ion formed from diethylamine represents a R.I. = 76.82% at 70 eV and 41.5% at 14 eV and from triethylamine represents a R.I. = 21.2% at 70 eV and 6.2% at 14eV.

All DFD IE curves for $[CH_4N]^+$ ions produced from the precursors show a small tail at threshold (Figs.9-11).

5.2.3.1. $[CH_4N]^+$ (m/z=30) Fragment Ion Obtained from Ethylamine:

The AE at threshold for $[CH_4N]^+$ produced from ethylamine is measured at 9.76±0.07 eV. This value is in good agreement with those measured early (Table 3) by Chupka[18] and by Lossing et al[15] but lower by 0.44 eV than the value reported also early by Collin et al[16]. The most obvious way to form $[CH_4N]^+$ ion from the precursor is a simple bond cleavage of CH_3 leading to the formation of the ion with the most stable structure (a) (scheme 1).

$$CH_3 - CH_2 - \overset{+\cdot}{N}H_2 \xrightarrow{-CH_3} CH_2 = \overset{+}{N}H_2$$

(a)

Scheme (1)

Assuming the lowest energy of m/z=30 ion has (a) $[CH_2NH_2]^+$ structure, then the calculated thermodynamical threshold (ΔE_{th}) value for the ion produced from ethylamine is 9.76 eV . The present experimental AE value for the ion is very close to the calculated thermodynamical threshold ($\Delta E_{th.}$) value for the formation of the most stable ion with structure (a), suggesting ε_{excess} = o. This is expected since the process of formation proceeds with 0.81 eV only above the ionization energy of ethylamine. It is worthnoting that no metastable peak was observed for the process of formation. On the other hand, if one assumes the formation of the fragment ion obtained from ethylamine at threshold with the less stable $[CH_3NH]^+$ structure, ΔE_{th} value will be equal to 10.54 eV. This value is higher by 0.78 eV than experimental AE at threshold which rules out the formation of the ion with structure $[CH_3NH]^+$.

5.2.3.2. The $[CH_4N]^+$ (m/z=30) Fragment Ion Obtained from Diethylamine.

The AE at threshold for $[CH_4N]^+$ ion produced from diethylamine is measured at 12.12 eV. This value is lower by about 1eV than the early reported value by Collin and Franskin[17]. The latter value probably do not correspond to the first AE of $[CH_4N]^+$ ion.

There are two possible processes (2 and 3) (Table3) leading to $[CH_4N]^+$ formation from the precursor, which is accessible in the energy range considered i.e. 3 eV above threshold. The lowest energy process is due to n-C_3H_7 loss (process 2) whereas the higher energy process (3) is due to successive loss of $CH_3^{\cdot}$ and C_2H_4 from the molecular ion of diethylamine. Process 3 is partially confirmed by the detection of metastable peak corresponding to the transition $[C_3H_8N]^+ \rightarrow [CH_4N]^+$,while for process 2 no metastable peak was observed. On the other hand, the calculated $\Delta E_{th.}$ values (for both structures a and b) for the formations of the ions according to processes 2 and 3 together with AE values at threshold (Table 3) rule out the formation of $[CH_4N]^+$ ions (with both a and b structures) at the measured threshold according to process 2 i.e. the ion is formed at threshold from the precursor according to process 3 by successive loss of $CH_3^{\cdot}$ and C_2H_4(scheme 2). Therefore, one may assume that the lowest energy process 2 did not occur at threshold. The calculated $\Delta E_{th.}$ values (Table 3) for the $[CH_4N]^+$ formation (with both structures a and b) according to process 3 reveal that the ion is formed at threshold with the less stable methylnitrinium (b) structure associated with ε_{excess}=o.65 eV.

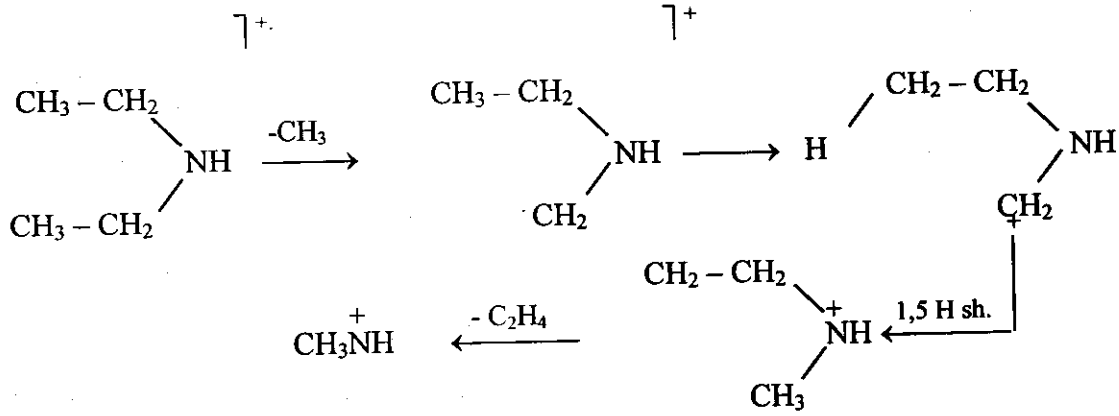

Scheme (2)

On the other hand, the KER ($T_{0.5}$)value with the ion formation is found to be 0.038 eV at 15 eV (nominal) (Table 6) . Assuming $\varepsilon_{excess} = \varepsilon^r_o$ and $T_{0.5} = T^e$ (it has been suggested previously that $\varepsilon^{\ddagger}$ may be neglected if $\varepsilon^r_o > 0.5eV$[140]) we calculated the energy partitioning quotient for the system $T_{0.5}/\varepsilon^r_o$ = 0.038/0.63 ≈0.06. This value corresponds to a rearrangement via a five-membered cyclic transition state[2,60] which is consistent with the suggested mechanism (scheme 2).

5.2.3.3. $[CH_4N]^+$ (m/z=30) Fragment Ion Obtained from Triethylamine.

The AE at threshold for $[CH_4N]^+$ ion produced from triethylamine is measured at 13.44 eV. The formation of the ion from triethylamine proceeds by two secondary decomposition processes (Table 3): process 4 by successive loss of CH_3+2-C_4H_8 and process 5 by successive loss of CH_3 +C_2H_4 +C_2H_4. Process 4 is partially confirmed by the detection of metastable peak corresponding to the transition $[C_5H_{12}N]^+ \rightarrow [CH_4N]^+$ (second step in process 4) with $T_{0.5}$= 0.103 eV. Also, process 5 is partially

confirmed by the detection of metastable peak corresponding to the transition $[C_3H_8N]^+ \rightarrow [CH_4N]^+$ (last step in process 5) with $T_{0.5}$= 0.039 eV at 15 eV. The calculated ΔE_{th} values for the ions formation (with both structures a and b) according to processes 4 and 5 (Table 3) together with the measured AE value at threshold (Table 3) rule out the formation of [CH_4N]+ ions at the detected threshold according to process 4 i.e. the lowest energy process 4 did not occur in this study and the ion is formed according to process 5 only. Hence, one propose that the metastable peak for the second step in process 4 may not be directly related to the present experiment, since it vanishes at energy higher than the measured AE at threshold. In contrast the metastable peak corresponding to the transition $[C_3H_8N]^+ \rightarrow [CH_4N]^+$ (last step in process 5) vanishes at energy lower than the AE measured at threshold.

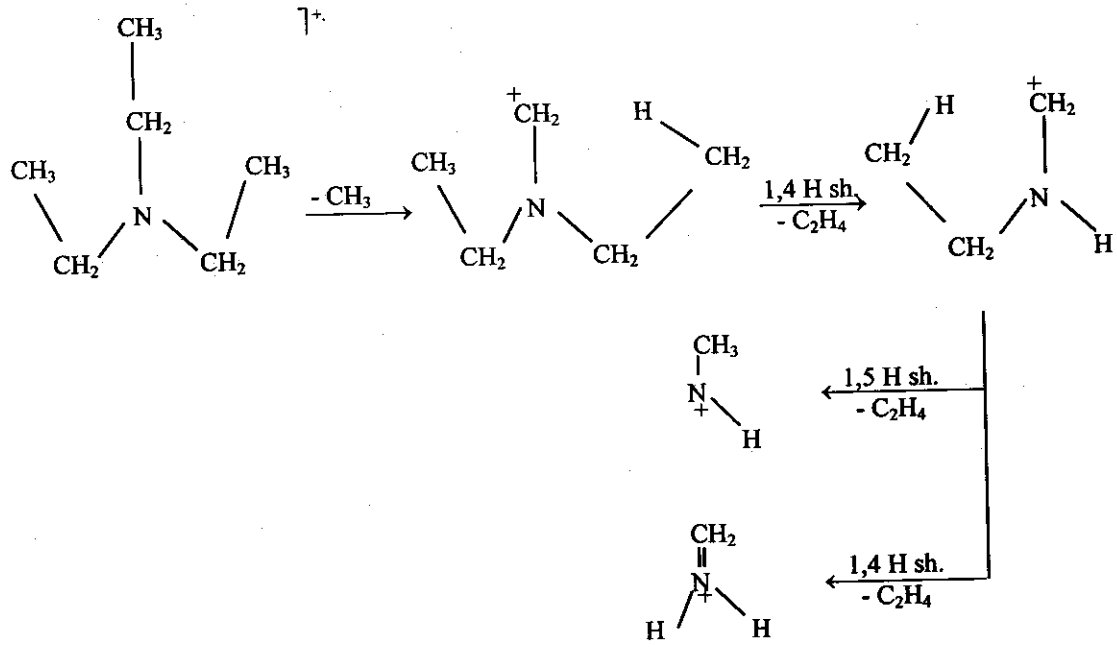

Scheme (3)

The calculated ΔE_{th} values (Table 3) for the formation of $[CH_4N]^+$ ions (with both structures a and b) according to process 5 indicate that the ion is formed at the detected threshold having the methylnitrinium structure (b) associated with $\varepsilon_{excess} = 1.22$ eV. Assuming $\varepsilon_{excess} = \varepsilon'_o$ and $T_{0.5} = 0.039$ eV $= T^e$ we calculated the energy partitioning quotient for the system as $0.039/1.22 \approx 0.03$.

This quotient is consistent with the mechanism (scheme 3) suggested for the formation of the ion from triethylamine with structure b which involve a rearrangement via a five-membered cyclic transition state[2,60].

5.2.4. The $[C_2H_6N]^+$ (m/z=44) Fragment Ion

The $[C_2H_6N]^+$ (m/z=44) fragment ion is prominent in the mass spectra of several amines and has been, therefore, the subject of many experimental[134,135,142,143,15,19] and theoretical studies[144-148]. $[C_2H_6N]^+$ ion can exists in two stable non-interconverting immonium structure (a and b) Much less stable structures (c-g) had been found to exist[15,19].

$CH_3CH = \overset{+}{N}H_2$ (a)

$CH_3\overset{+}{N}H = CH_2$ (b)

$H_2C = CH\text{-}\overset{+}{N}H_3$ (c)

$CH_2 - \overset{+}{N}H_2 - CH_2$ (d)

$\dot{C}H_2\ CH_2\ \overset{+}{N}H_2$ (e)

$CH_3\overset{+}{N}CH_3$ (f)

$CH_3CH_2\overset{\cdot +}{N}H$ (g)

Several studies[9,17,149-151] have determined appearance energies (AE,s) of $[C_2H_6N]^+$ ions from various precursors, but these results have been inconclusive regarding any relationship between ΔH_f and the structure of $[C_2H_6N]^+$ isomers. Solka and Russell[19] used the calculated heats of formation values (from measured AE values) of $[C_2H_6N]^+$ ions resulting from the fragmentation of a variety of amines as a tool in characterizing the structural isomers of $[C_2H_6N]^+$.

All the DFD IE curves for $[C_2H_6N]^+$ ions produced from ethylamine, diethylamine and triethylamine show a slow rise at threshold (Figs.12-14).

The $[C_2H_6N]^+$ fragment ion represents one of the low abundance ion in the mass spectra of the three precursor. For ethylamine, the ion represents 22.96% at 70 eV and 6.24% at 14 eV, while for diethylamine represents 26.42% at 70 eV and 7.77 at 14 eV, for triethylamine represents 10.44% at 70 eV and 1.11% at 14 eV Table (1).

$[C_2H_6N]^+$ (m/z=44) fragment ion obtained from ethylamine

The presently measured AE at threshold produced from ethylamine is measured at 9.63±0.07eV. This value of AE at threshold is in agreement with those measured by Lossing et al[15] (9.55 eV), by Solka et al[19] (9.61eV) and is lower by 2.27eV than the value reported by Collin[16] (Table 4).

The $[C_2H_6N]^+$ ion may be formed by loss of α-hydrogen atom as shown by Collin,s[139] study for $CH_3CD_2NH_2$ forming ethaniminium structure (process 1a) or by loss of β-hydrogen atom forming unstable β-aminoethyl cation (process 1b) .

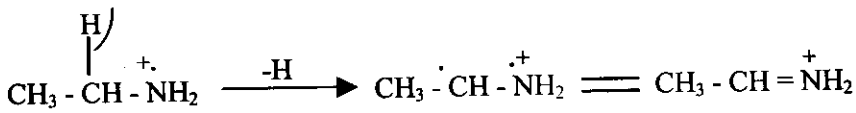

(1a)

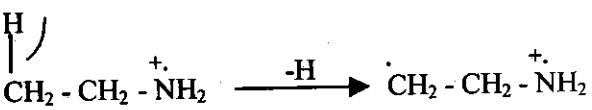

(1b)

Scheme (1)

Assuming the formation of isomer $[a]^{+\cdot}$ (ethaniminium ion) from ethylamine (by process **1a)** and using thermodynamical considerations together with AE value indicate that the ion formed with the most stable ethaniminium structure $[a]^+$ associated with 0 eV excess energy. This is expected since the process of formation proceeds with $\varepsilon_0 = 0.68$ eV only above the ionization energy of ethylamine. It is worthnoting that no metastable peak is observed for the process of formation. On the other hand, for the formation of $[C_2H_6N]^+$ with structure $[e]^+$ (1b), ΔE_{th}=11.81eV which is higher than the AE value by 2.18 eV, indicating that the ion do not formed at threshold with structure $[e]^+$ but formed with the stable ethaniminium structure (a) (process 1a).

$[C_2H_6N]^+$ (m/z=44) fragment ion obtained from diethylamine

The AE at threshold for $[C_2H_6N]^+$ produced from ethylamine is measured at 11.46 $\pm$ 0.09 eV . This value is in a good agreement with the value (11.42 eV) reported by Solka and Russell[19] (Table 4) and is lower by 2.19 than the value obtained by Collin and Franskin[17] .

There are two possible decomposition processes (2 and 3) leading to $[C_2H_6N]^+$ ion formation from the molecular ion which are accessible in the considered energy range i.e. 3.5 eV above threshold. Rupture of C_2H_5 (process 2) or successive loss of H + C_2H_4 (process 3) are as follows:

$$CH_3CH_2 - \overset{+\cdot}{N}H - CH_2CH_3 \xrightarrow{-C_2H_5} CH_3CH_2 - \overset{+}{N}H \quad (2)$$

$$CH_3CH_2 - \overset{+\cdot}{N}H - CH_2CH_3 \xrightarrow{-H} CH_3CH = \overset{+}{N}H - CH_2CH_3 \xrightarrow{-C_2H_4} CH_3 - CH = \overset{+}{N}H_2 \quad (3)$$

Process 3 is partially confirmed by the detection of metastable peak which is corresponding to the transition $[C_4H_{10}N]^+ \rightarrow [C_2H_6N]^+$ (m*=26.88), while no metastable peak is observed for process 2. On the other hand, the calculated $\Delta E_{th.}$ values (for both structures a and g) for the formation of the ions according to process 2 and 3 together with AE values at threshold (Table 4) rule out the formation of $[C_2H_6N]^+$ ions at the measured threshold according to process 2 i.e. the ion is formed at threshold from the precursor according to process 3 by successive loss of H and C_2H_4 (not by the lowest energy process 2). The calculated $\Delta E_{th.}$ values (Table 4) for the $[C_2H_6N]^+$ formation (with structures a and g) according to process 3 reveal that the ion is formed at threshold with stable ethaniminium (a) structure associated with $\varepsilon_{excess} = 1.07eV$.

On the other hand, the KER ($T_{0.5}$) value associated with the ion formation (transition) is found to be 0.044 eV at 14eV (nominal) (Table 7). Assuming $\varepsilon_{excess} = \varepsilon^r_0$ and $T_{0.5} = T^e$ (it has been suggested previously that $\varepsilon^{\ddagger}$ may neglected if $\varepsilon^r_0 > 0.5$ eV[140]), the energy partitioning quotient for the system is calculated to be: $T_{0.5} / \varepsilon^r_0 = 0.044 / 1.07 \approx 0.041$. This value corresponds to a rearrangement via a five or six membered cyclic transition state[2,60].

$[C_2H_6N]^+$ (m/z=44) Fragment Ion Obtained from Triethylamine

The AE at threshold for $[C_2H_6N]^+$ produced from triethylamine is measured at 13.71 $\pm$ 0.07 eV . To our knowledge no similar experimental values in literature are found to compare with. Two possible processes of formation of $[C_2H_6N]^+$ ion from triethylamine are suggested, all of which

are secondary decomposition processes: successive loss of H+2-C_4H_8 (process 4) and successive loss of H+ C_2H_4 + C_2H_4 (process 5) . The formation of the ions according to process 4 and 5 at 14 eV are associated with metastable peaks having KER ($T_{0.5}$) = 0.096 eV ($[C_6H_{14}N]^+ \rightarrow [C_2H_6N]^+$) (2nd step) and $T_{0.5}$ = 0.042 eV ($[C_4H_{10}N]^+ \rightarrow [C_2H_6N]^+$) (third step), respectively.

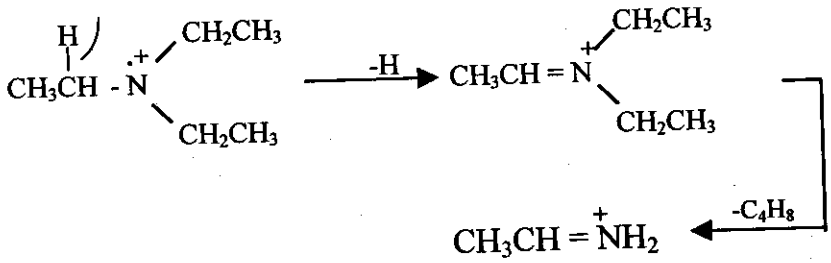

(4)

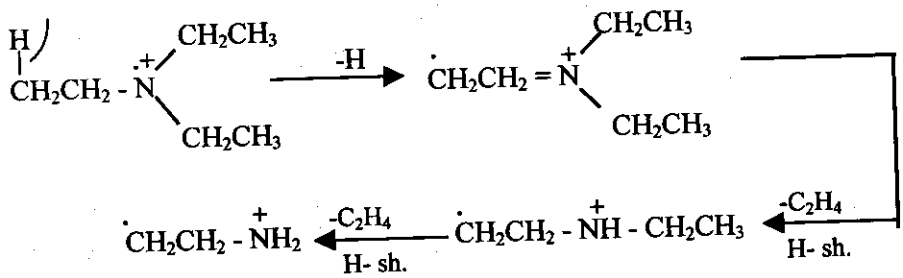

(5)

The calculated $\Delta E_{th.}$ values for the $[C_2H_6N]^+$ ions formation (with both structures a and e) according to process 4 and 5 (Table 4) together with the measured AE value at threshold rule out the formation of $[C_2H_6N]^+$ ions at threshold according to process 4, i.e. the lowest energy process 4 does not occur and the ion is formed according to process 5 only. It is noteworthy that the metastable peak corresponding to transition ($[C_6H_{14}N]^+ \rightarrow [C_2H_6N]^+$) (process 4, second step) vanishes at an energy higher than the measured AE value, while metastable peak corresponding to transition $[C_4H_{10}N]^+ \rightarrow [C_2H_6N]^+$ (last step in process 5) vanishes at an energy lower than AE measured at threshold. On the other hand, the

calculated $\Delta E_{th.}$ values (Table 4) for the formation of $[C_2H_6N]^+$ (with both structures a and e) according to process (5) indicate that the ion is formed at detected threshold having the β-aminoethyl structure $[e]^+$ associated with ε_{excess}=0.60 eV. Assuming $\varepsilon_{excess} = \varepsilon^r_0$ and $T_{0.5} = 0.042$ eV $= T^e$, we calculated the energy partitioning quotient for the system as $0.042/0.60 \approx 0.07$. This quotient is consistent with the mechanism suggested for the formation of the ion from triethylamine with structure e which may involve a rearrangement via a five membered cyclic transition state[2,60].

5.2.5. $[C_3H_8N]^+$ (m/z= 58) Fragment Ion:

Metastable ion spectra of $[C_3H_8N]^+$ ion have been studied by Uccella et al[134] and were reinvestigated by McLafferty[135]. $[C_3H_8N]^+$ ions, which according to the mechanism of formation have five initial structures (a–e) yield four distinct metastable ion spectra[1,3a] demonstrating that $[C_3H_8N]^+$ ions (a to c) with sufficient energy to decompose and a life time 10^{-6}s have distinct structures, while d and e rearrange to common structure or interconverting structures prior to further decomposition.

$CH_3CH_2CH=\overset{+}{N}H_2$ (a)

$CH_2=\overset{+}{N}H\ CH_2\ CH_3$ (b)

$(CH_3)_2C=\overset{+}{N}H_2$ (c)

$CH_3CH=\overset{+}{N}H\ CH_3$ (d)

$(CH_3)_2\overset{+}{N}=CH_2$ (e)

On the other hand, the possible isomerization / dissociation processes of immonium $[CH_3CH_2CH=NH_2]^+$ and $[CH_2=NH\ CH_2CH_3]^+$ ions have been discussed by Bowen[152].

The m/z=58 $[C_3H_8N]^+$ fragment ion represent the base peak in the mass spectrum of diethylamine at 70eV and at 14 eV, while for triethylamine the ion has moderate abundance 21.43% at 70 eV and 37.30% at 14eV (Table 1). The DFD IE curves for $[C_3H_8N]^+$ ions produced from the diethylamine and triethylamine show a slow rise at threshold (Fig.15-16).

$[C_3H_8N]^+$ (m/z= 58) Fragment Ion Obtained from Diethylamine:

The experimental appearance energy (AE) at threshold of $[C_3H_8N]^+$ ion obtained from diethylamine is measured at 9.06±0.07 eV, which is in a good agreement with the value reported in the literature by Lossing et al[15] at 8.92 eV using an energy resolved electron beam. The most obvious way to form $[C_3H_8N]^+$ ion from the molecular ion is a simple bond cleavage of CH_3 leading to the formation of the ion with the most stable structure(b).

$$CH_3 - CH_2 - \overset{+.}{N}H - CH_2 - CH_3 \xrightarrow{-CH_3} CH_2 = \overset{+}{N}H - CH_2 - CH_3 \qquad (1)$$

Assuming the $[C_3H_8N]^+$ fragment ion formed at threshold with both structure a and b with ΔH_f =636 kJ mol^{-1}[15] and ΔH_f=653 kJ mol^{-1}[15]. Combining these with ΔH_f $[CH_3]$=145.8 kJ mol^{-1}[136] and ΔH_f $[C_4H_{11}N]^{+\cdot}$ =75.35 kJ mol^{-1}[136] yields a calculated thermodynamical threshold (ΔE_{th}) values at 8.88 (a) and 9.069 (b) eV, associated with excess energy at 0.18 (a) and 0 eV (b).

The experimental AE for the ion is very close to the calculated thermodynamical threshold (ΔE_{th}) value for the formation of $[C_3H_8N]^+$ with structures (b) with the lowest excess energy (ε_{excess} =0 eV). This is expected since the process of formation of $[C_3H_8N]^+$ from the molecular ion is a simple cleavage.

$[C_3H_8N]^+$ (m/z= 58) Fragment Ion Obtained from Triethylamine:

The experimental appearance energy (AE) value for $[C_3H_8N]^+$ fragment ion obtained from triethylamine at threshold is equal to

9.92±0.09 eV. To the best of the author knowledge, no AE values for $[C_3H_8N]^+$ ions produced from the triethylamine were previously published.

There are two possible processes (2 and 3) leading to $[C_3H_8N]^+$ formation from the precursor which are accessible in the energy range considered i.e. 3 eV above threshold.

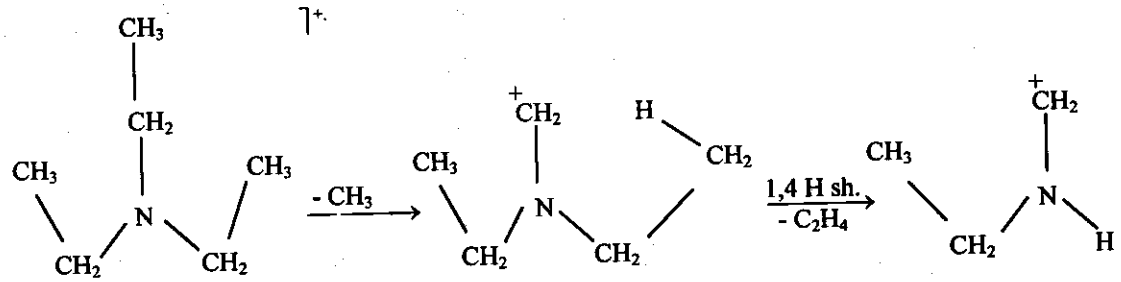

Scheme (2)

The lowest energy process is due to n-C_3H_7 loss (process 2) whereas the higher energy process (3) is due to successive loss of $CH_3^{\cdot}$ and C_2H_4 from the molecular ion of triethylamine. Process 3 is partially confirmed by the detection of metastable peak corresponding to the transition $[C_5H_{12}N]^+ \rightarrow [C_3H_8N]^+$ (m^* =39.1), while for process 2 no metastable peak was observed. On the other hand, the calculated $\Delta E_{th.}$ values (for both structures a and b) for the formations of the ions according to processes 2 and 3 together with AE values at threshold (Table 5) rule out the formation of $[C_3H_8N]^+$ ions (with both a and b structures) at the measured threshold according to process 2i.e. the ion is formed at threshold from the precursor according to process 3 by successive loss of $CH_3^{\cdot}$ and C_2H_4. The calculated $\Delta E_{th.}$ values (Table 5) for the $[C_3H_8N]^+$ formation (with both structures a and b) according to process 3 reveal that the ion is formed at threshold with the ethylmethaniminium structure $[CH_3\,CH_2NH{=}CH_2]^+$ (b) associated with ε_{excess}= o.35 eV.

5.2.6. Kinetic Energy Releases ($T_{0.5}$) and the Structure of the Reactive Metastable Fragment Ions:-

The measurements of kinetic energy release ($T_{0.5}$) during fragmentation of metastable ions are a technique which is frequently used as a probe of ion structure[2,153]. If the kinetic energy release ($T_{0.5}$) is determined from metastable peak width, then the fact that the mass spectrometer detects as metastable ions only these which fragment in a specified narrow time interval means that the excess energies, $\varepsilon^{\ddagger}$, are quite closely fixed by the instrumental conditions[2]. Hence, whether or not ε^{r}_{o} makes a major contribution to T, the kinetic energy released will be less sensitive to internal energy and more sensitive to ion structure than are other parameters of metastable ions including their abundances. Thus by comparison of ions formed from different sources, for example by fragmentation of different molecular ions, it should be possible to determine from the kinetic energy released ($T_{0.5}$) in their further fragmentation whether or not they are identical, even if they do not have the same internal energy distribution.

The present author uses the kinetic energy release ($T_{0.5}$) in fragmentation of $[CH_4N]^+$, $[C_2H_6N]^+$ and $[C_3H_8N]^+$ ions as a parameter for probing their ionic structures.

The Reactive $[CH_4N]^+$ Fragment Ions:

The kinetic energy release ($T_{0.5}$) values associated with fragmentation of $[CH_4N]^+$ ions obtained from the precursors at 70 eV (Table 6) according to the following transition:

$$[CH_4N]^+ \rightarrow [CH_2N]^+ + H_2$$